The challenges of accelerated aging techniques for elastomer lifetime predictions – Part 1

K. T. Gillen, R. Bernstein, M. Celina

Elastomers are often degraded when exposed to air or high humidity for extended time periods (years to decades). Lifetime estimates normally involve extrapolating accelerated aging results made at higher than ambient environments. Several potential problems associated with such studies are reviewed and experimental/theoretical methods to address them are provided. The importance of verifying time-temperature superposition of degradation data is emphasized as evidence that the overall nature of the degradation process remains unchanged versus acceleration temperature. The confounding effects that occur when diffusion-limited oxidation (DLO) contributes under accelerated conditions are described and it is shown that the DLO magnitude can be modeled by measurements or estimates of oxygen permeability coefficients (P_{0x}) and oxygen consumption rates (ϕ) . P_{0x} and ϕ measurements can be influenced by DLO and it is demonstrated how confident values can be derived. Additionally, several experimental profiling techniques that screen for DLO effects are discussed. Values of ϕ taken from high temperature to temperatures approaching ambient can be used to more confidently extrapolate accelerated aging results for air-aged materials and many studies now show that Arrhenius extrapolations bend to lower activation energies as aging temperatures are lowered. Best approaches for accelerated aging extrapolations of humidity-exposed materials are also offered. Part 1 covers the timetemperature superposition approach (chapter 2) and diffusion-limited oxidation (DLO) complications (chapter 3).

1 Introduction

Elastomers are often expected to last for decades under various air containing environments. Confirming such extended lifetimes requires accelerated aging approaches. The most common method is to extrapolate degradation results from accelerated aging studies conducted at higher than ambient conditions (e.g., accelerated aging tempera-

Kenneth T. Gillen dandkgillen@comcast.net Robert Bernstein, Mat Celina

Sandia National Laboratories, Albuquerque, NM, USA

Published with kind permission of The Rubber Division, American Chemical Society, Inc.; Akron, OH, USA

tures). The extrapolations are normally modeled using the Arrhenius approach [1] which is supposed to reflect the temperature dependency of the chemistry underlying the degradation processes. Unfortunately, this general approach can be misguided with many potential problems that are the subject of this review. One potential problem involves changes in the dominant chemical degradation pathway as the temperature is changed, implying that the chemistry extrapolated from the accelerated high temperature aging conditions may not reflect the chemistry occurring under lower temperature ambient aging conditions. Similarly, the correlation between degradation levels (oxidation extent) and mechanical properties, the primary goal of many predictive aging studies may depend on temperature. A second problem involves physical (geometric and material depth) effects caused by the potential presence of diffusion-limited oxidation (DLO) [2-5]. DLO occurs when oxidation reactions in the cross-section of a material use up oxygen faster than it can be

replenished by diffusion from the surrounding air atmosphere. This leads to equilibrium oxidation at the air-exposed sample surfaces but diminished or non-existent oxidation away from the surface. Since oxidation normally dominates chemical degradation mechanisms, the presence of DLO effects will lead to a diminished average degradation rate. Since DLO effects become more important as the temperature is increased, they can have a large impact on accelerated exposures, but may not contribute under ambient conditions, making any attempted extrapolation of limited value. The impact of DLO on the feedback from multiple experimental approaches under thermo-oxidative conditions has recently been reviewed [6].

This paper will review some of the approaches we have taken to address these challenges such that more confident lifetime predictions can be generated. To screen for evidence of changing degradation chemistry with changes in temperature, we will describe the use of time-temperature (t-T) superposition, as well as the use of ultrasensitive oxygen consumption methods that are capable of taking measurements down to very low aging temperatures (often to ambient). It will also be shown how temperature-dependent DLO effects can be modeled and understood through temperature-dependent measurements of oxygen permeability and oxygen consumption rates and how these effects can be experimentally monitored through the use of various profiling techniques. Finally, we will show how predictions can be made for humidity sensitive materials.

2 Time-temperature superposition approach

Many accelerated aging approaches involve following a property associated with degradation at several elevated temperatures and modeling the time to a certain amount of damage at each temperature in order to obtain a functional form of the temperature-dependent damage. This functional form is then extrapolated to lower temperatures representative of ambient aging conditions to make predictions for these conditions. An example of such an approach

comes from studies of an EPDM o-ring where various properties (tensile elongation, density, modulus, sealing force) showed little change until very large changes quickly occurred at the end of the so-called induction time. When the log of the induction times for all four variables was plotted versus inverse absolute aging temperature, linear behavior resulted as seen in **figure 1**.This linear behavior is consistent with the Arrhenius model that states that t – the aging time of interest (induction-time in the current example) – is given by **equation 1**:

$$t \propto exp \left[\frac{-E_a}{RT} \right]$$
 1

 $\rm E_a$ is the Arrhenius activation energy, R is the gas constant and T is the absolute aging temperature in degrees Kelvin. As seen in **figure 1**, $\rm E_a$ is equal to ~116 kJ/mol for this material. Clearly if $\rm E_a$ remains constant down to ~25 °C, an extremely long life (~55,000 years) is predicted at this temperature. However, given the extended extrapolation regime relative to the aging temperature range examined, very little confidence exists in this extrapolation.

A major problem with such approaches is the possibility that the important degradation reactions differ as a function of aging temperature. When two different reactions with differing E_a values are important to the degradation over the temperature range of interest (e.g., accelerated range and the extrapolation range), the reaction with a lower activation energy will become more important and then dominant as T drops. This is illustrated in figure 2, where the overall solid line degradation curve follows the high E_a process at high temperatures and transitions to the low E_a process as the temperature is reduced. Thus, if changes occur in Arrhenius slopes, one normally expects changes to lower slopes (lower Ea values), which has been observed for multiple materials [6].

We clearly need approaches capable of recognizing the possibility of changing chemistry over the temperature range of interest. One method of particular utility for discovering chemistry changes occurring in the temperature range encompassing the accelerated temperature exposures involves time-temperature (t-T) superposition [1, 7]. This method will be described in this section. Later, we will discuss a second method involving ultrasensitive oxygen consumption techniques that allow us to probe the extrapolation regime looking for possible changes in Arrhenius slope.

Time-temperature superposition concepts have been used for many decades to enable thermal aging predictions at experimentally inaccessible times [8]. The important concept is that instead of using one data point from each accelerated temperature (e.g., the induction time, the time to 50 % tensile elongation, etc.), this approach uses all of the time-dependent data generated at each aging temperature [1, 7]. An example of normalized tensile elongation data [9] for a nitrile rubber material is shown in **figure 3**.

If raising the accelerated aging temperature speeds up the degrading chemical reaction without changing the reactions, the degradation curves at the two temperatures will be related by a constant multiplicative factor, referred to as the shift factor a_T. This implies that the shape of the curves should be similar when plotted versus log time as is the case for the nitrile data shown in figure 3. Time-temperature superposition uses this concept by selecting a reference T, often the lowest accelerating temperature (64.5 °C in the present case) and finds the multiplicative shift factor for each higher T needed to shift the higher temperature results for the best superposition of the results. By definition the value of a_T at the reference T is 1. The multiplicative shift factor a_T that achieves

Fig. 1: Arrhenius plot of induction times for an EPDM o-ring material

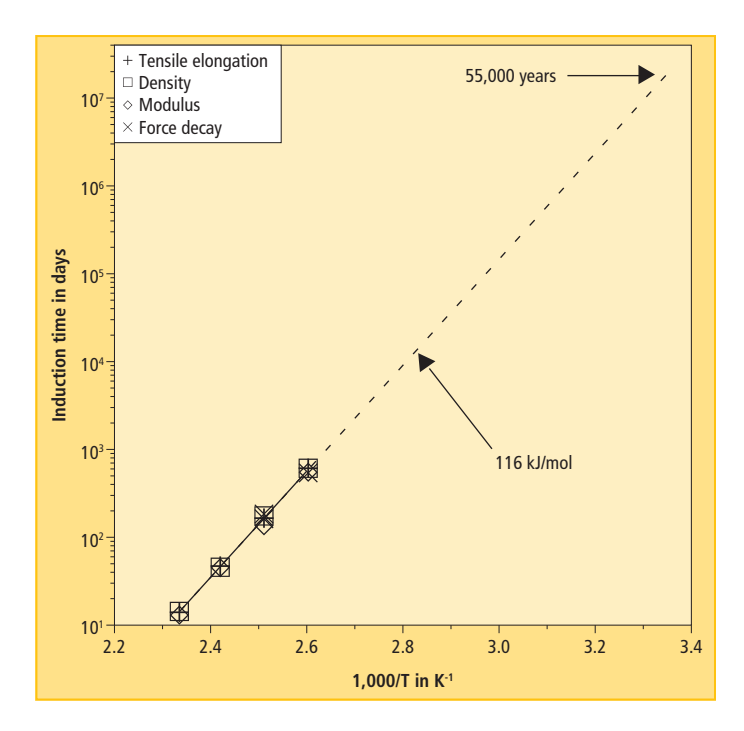
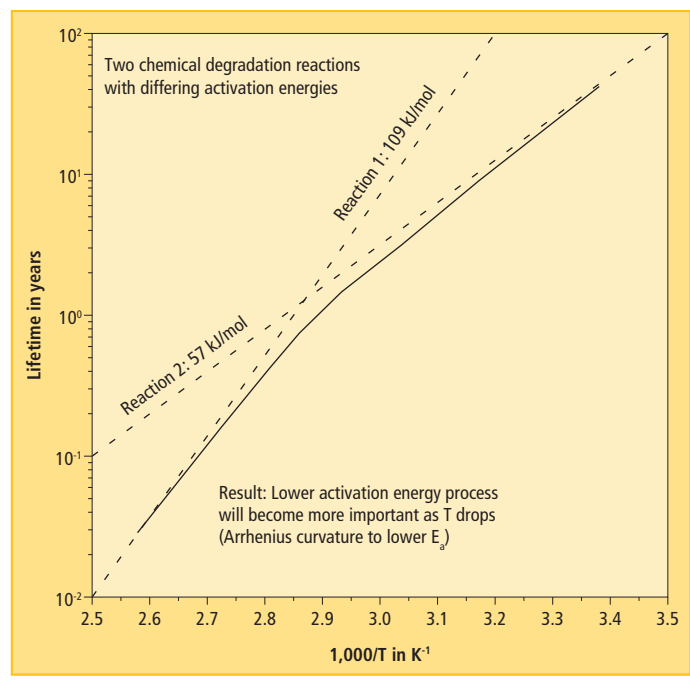


Fig. 2: Hypothetical results when two different degradation reactions represent material degradation over a large temperature range



the best superposition of the 80 °C results with the 64.5 °C results is a factor of 3.7 as indicated in **figure 3** by the horizontal lines representing a multiplicative time-factor of 3.7 given in the figure. The data from the remaining temperatures are shifted in a similar fashion to give the best overall superposition with the final superposed results shown in **figure 4.**

The excellent superposition gives compelling evidence that the same chemical degradation pathway dominates the entire temperature range of the accelerated experiments. Instead of using one data point per aging temperature in the analysis, t-T superposition uses every data point and is therefore a clearly preferred approach. The resulting \mathbf{a}_{T} factors can now be plotted for

the nitrile rubber on an Arrhenius plot (fig. 5) and the results yield linear Arrhenius behavior with an E_a of ~90 kJ/mol. By extrapolating the results to 25 °C, we obtain a shift factor of ~0.014, implying lifetimes ~70 times greater than those determined at 64.5 °C. Therefore if "failure" is considered to be when the elongation reaches 25 % of initial (~1.5 years from figure 4), lifetimes

Fig. 3: Normalized elongation data for a commercial nitrile rubber versus aging time at five accelerated aging temperatures

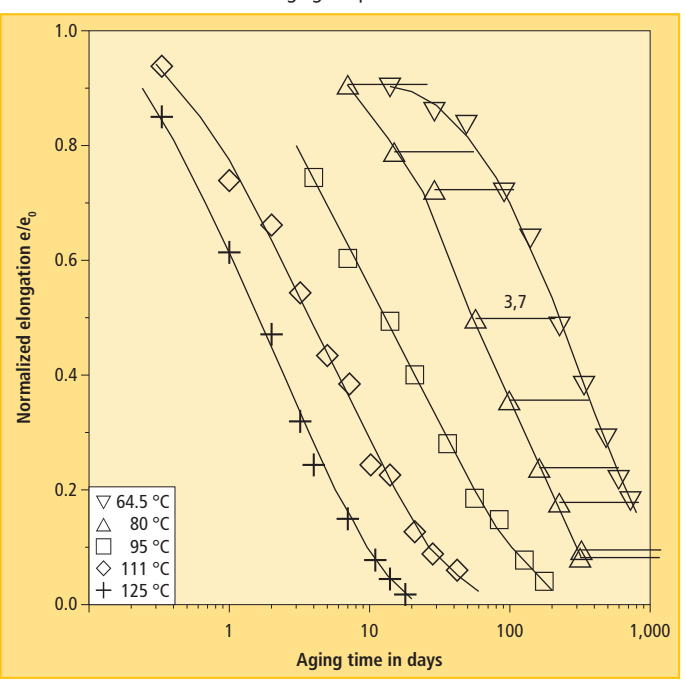


Fig. 4: Time-temperature superposition of data from previous figure

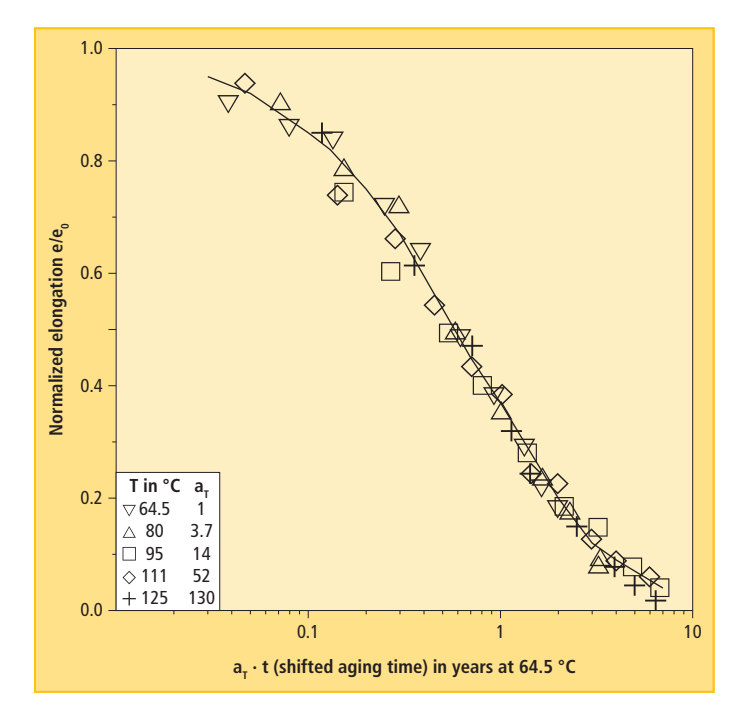


Fig. 5: Arrhenius plot of the shift factors for nitrile rubber from figure 4

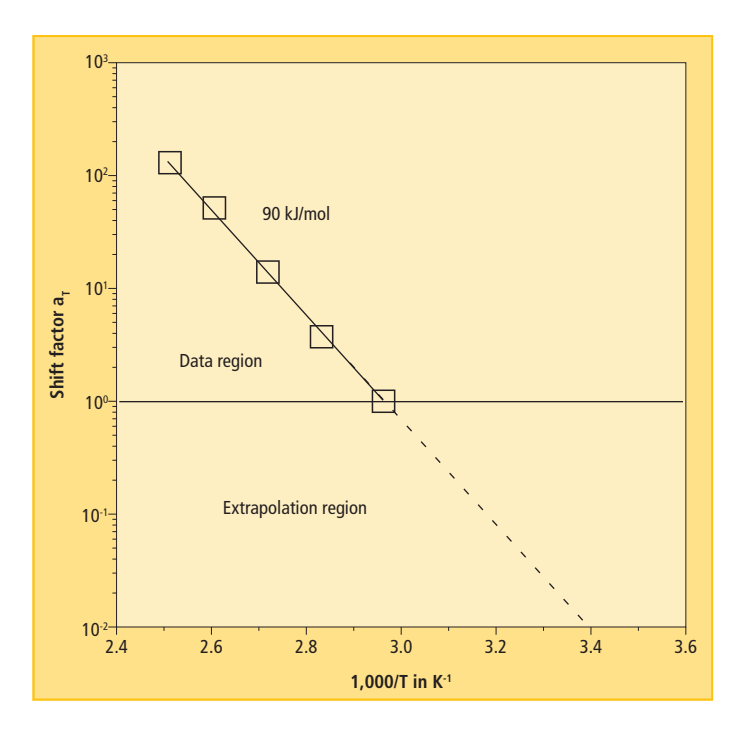
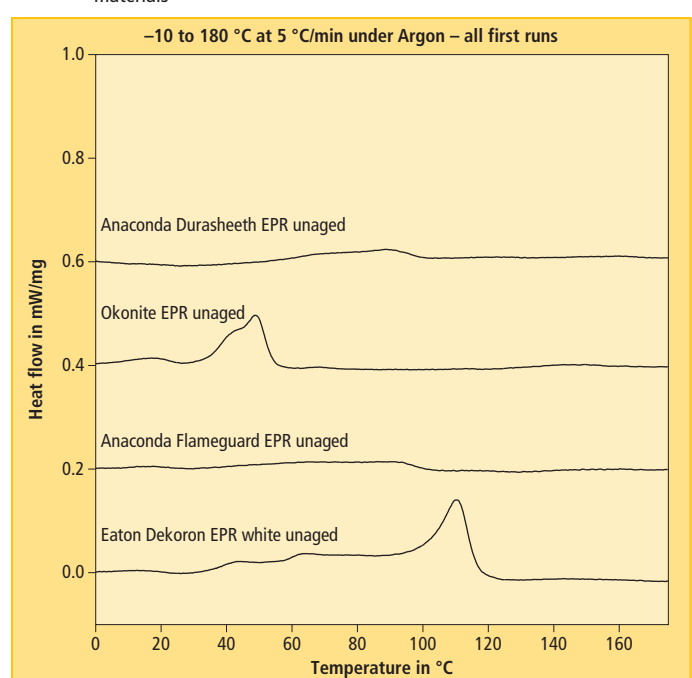


Fig. 6: DSC scans of four unaged commercially formulated EPR cable insulation materials



approaching 100 years would be predicted at 25 °C. Of course this assumes that the $\rm E_a$ does not drop in the extrapolation region (lower than 65 °C), an assumption that will be examined later.

Using t-T superposition analyses allows a quick evaluation of whether there is any evidence of chemistry changes in the accelerated aging temperature regime. An interesting example [10] compares two commercial EPR cable insulation materials both manufactured by Anaconda. DSC scans of these two materials are shown in **figure 6**, in comparison with some other EPR materials.

As opposed to the other two commercial cable materials, the DSC scans of Ana-

conda Flameguard EPR and Anaconda Durasheeth EPR show little evidence of crystallinity. Time-temperature superposition of tensile elongation results [10] over similar aging temperature ranges, are shown in figure 7 (Anaconda Flameguard EPR) and figure 8 (Anaconda Durasheeth EPR utilizing the 50 % elongation point for superposition). Clear evidence of changes in chemistry

Fig. 7: Time-temperature superposition of tensile elongation results for Anaconda Flameguard EPR

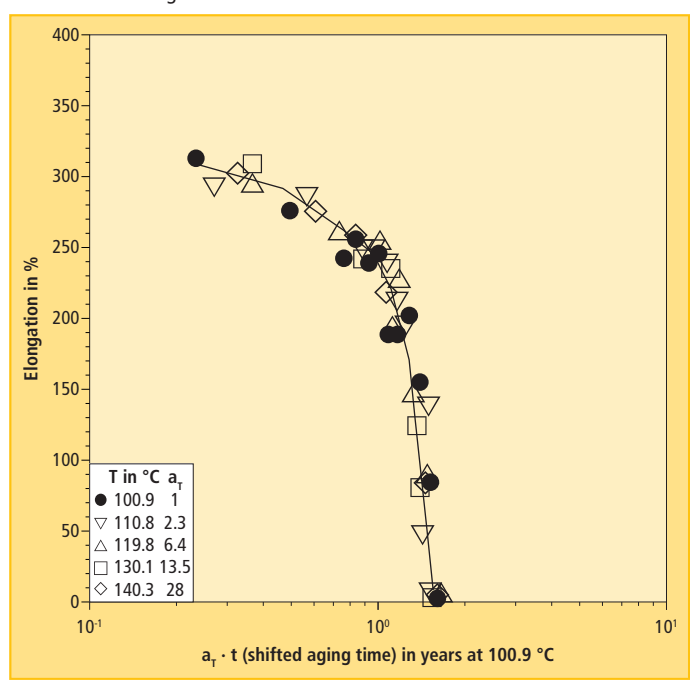


Fig. 9: DSC scan of a commercially formulated Brandrex XLPO cable insulation material

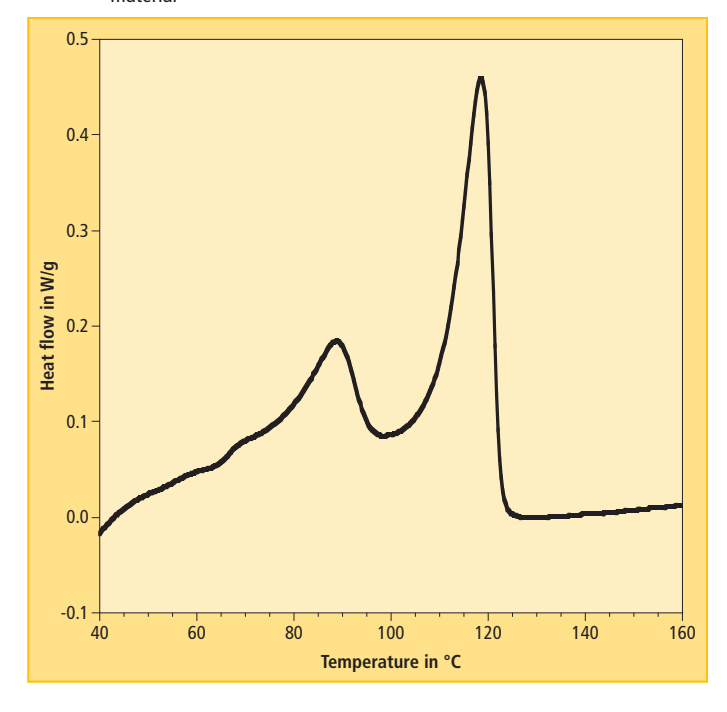


Fig. 8: Time-temperature superposition of tensile elongation results for Anaconda Durasheeth EPR

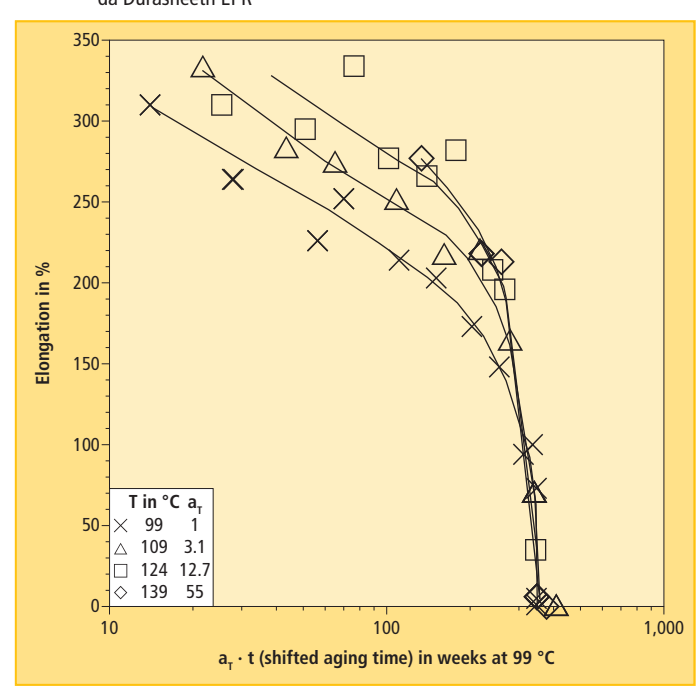
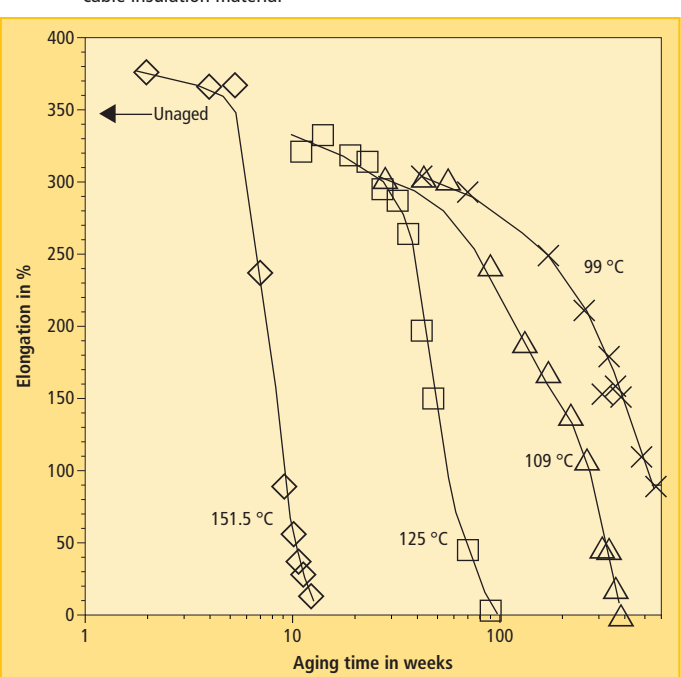


Fig. 10: Tensile elongation results versus aging temperature for a Brandrex XLPO cable insulation material



with aging temperature exists only for the Durasheeth material.

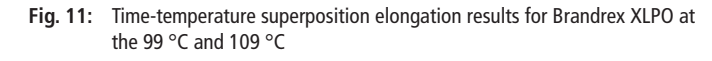
The tensile elongation results for a commercially formulated XLPO cable insulation material with a complex crystalline melting point region (fig. 9) are shown in figure 10 [11]. Since the shapes of the elongation curves above the main melting peak (~115 °C) differ dramatically from the results at 99 °C and 109 °C, it suggests the chemistry (or the correlation between degradation chemistry and mechanical properties) occurring above the main peak differs from that occurring below this peak, so t-T superposition analyses would not be appropriate. The shapes of the 99 °C and 109 °C curves are similar and reasonable t-T superposition of these curves is found as seen in figure 11. The examples shown in this section illustrate the power of t-T superposition in determining whether chemistry changes occur under accelerated temperature aging conditions.

3 Diffusion-limited oxidation (DLO) complications

When air surrounds polymers during aging, oxygen is dissolved in the materials. The equilibrium dissolved oxygen concentration

for each material is given by the product of its oxygen solubility coefficient S times the oxygen partial pressure p surrounding the polymer (Henry's law $S \cdot p$). Aging will cause the dissolved oxygen to be used up by oxidation reactions. If these reactions occur faster than diffusion processes from the surrounding air atmosphere can replenish the dissolved oxygen, the concentration of oxygen in the polymer interior will be reduced from its equilibrium value to lower or even non-existent levels. This effect can lead to diffusion-limited oxidation (DLO) effects, where the rate of oxidation is reduced or eliminated within the material. The importance of DLO effects depends on the material (physical and chemical behavior), its geometry (thickness) and its aging environment. For the relatively short-term accelerated aging conditions (days to months) applied to most elastomers, DLO effects are typically significant, leading to a partially oxidized material. As we will see shortly, DLO effects become less important as the accelerated aging temperature drops. In most cases, DLO effects will become unimportant under the slow oxidation conditions occurring for long-term, low-temperature ambient aging, implying uniform equilibrium oxidation across the entire cross-section of the elastomer. Clearly it is intrinsically risky to model high-temperature accelerated aging conditions influenced by geometry-dependent and temperaturedependent DLO effects in order to extrapolate the models to lower temperature non-DLO ambient conditions.

There is considerable literature available on modeling of DLO effects [2, 3, 12] and successful quantitative confirmations of the models [3, 12, 13]. For the purposes of this review, it is noted that detailed discussions of these models are available, but go beyond our current needs. For the current discussions concentrating on uniform thickness sheet material surrounded by air on both sides, we note that the models lead to predictions of the oxidation profile across the sample cross-section. The models require measurements or estimates of the oxygen permeability coefficient Pox and the oxygen consumption rate φ under the environmental conditions of interest, plus an estimate of how ϕ depends on oxygen partial pressure, p. A simple expression from the modeling [7] allows one to quickly estimate the maximum sheet thickness allowed before important DLO effects enter. The expression calculates L₉₀, the sheet thickness in which the integrated oxidation across the sample thickness is at least 90 % of its surface equivalent (e.g., minimal DLO



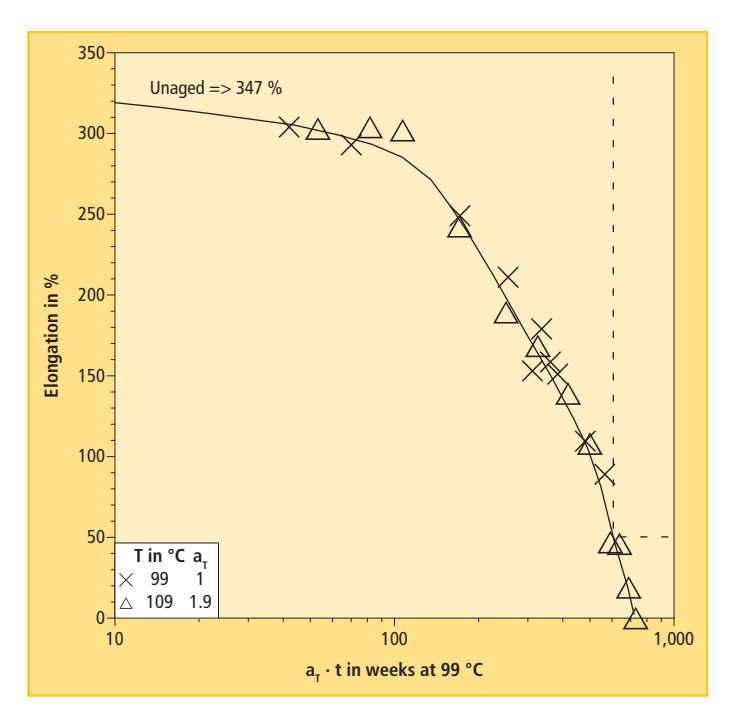
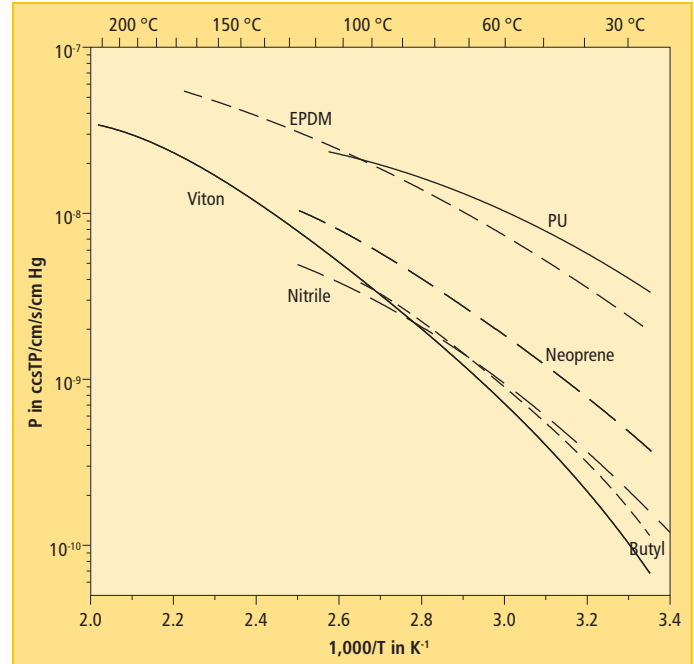


Fig. 12: Temperature dependence of P_{ox} versus inverse absolute temperature for various elastomers (ccSTP: cubic centimeters of gas at standard temperature and pressure)



effects with nearly uniform degradation, equation 2):

$$L_{90} \approx \left[\frac{kpP_{0x}}{\varphi}\right]^{0.5}$$
 2

where p is the oxygen partial pressure surrounding the sample and k is a constant that is typically found to be around 2 for air aging of elastomers [3, 12].

Equation 2 is very useful for understanding how DLO effects depend on aging temperature by comparing the temperature dependencies of ϕ and P_{0x} . The presence of oxygen during thermal aging invariably results in the degradation being dominated by oxidation chemistry. Thus the Arrhenius activation energy E_a for the oxygen consumption rate ϕ is typically strongly related to the E_a found for the degradation variable being monitored (such as tensile elongation). Most degradation E_a values are in the range from 70 to 130 kJ/mol. At low temperatures, literature on the temperature dependence of P_{0x} values for elastomers indicate E_a values in the range from 30 to 50 kJ/mol [14]. However, until recently, few measurements of P_{0x} have been made at the higher temperatures typically used in accelerated aging studies. This is because such measurements were difficult to make since they are easily convoluted by important DLO effects. By careful modeling of the DLO effects occurring, a recent study [14] succeeded in obtaining both low and high temperature Pox measurements for several elastomeric materials as shown in figure 12. As indicated in this figure, the Arrhenius plots indicated curvature of Pox to even lower E_a values (15 to 30 kJ/mol) at higher temperatures. Since φ increases much faster with increasing temperature than P_{0x} , equation 2 implies that DLO effects become less important with decreasing temperature. It should also be noted that in the later stages of the degradation of a material, φ may begin to increase and P_{0x} may decrease [12] both of which can lead to an increase in the importance of DLO effects.

One approach towards determining the importance of DLO effects is to use various experimental profiling techniques to map property variations across the cross-section of the aged material. There are numerous useful profiling techniques [15] and we will describe some typical data from one approach developed at Sandia. This approach involves the use of a modulus profiler that allows quantitative modulus values to be obtained across the cross-section of a material with 50 µm resolution [16, 17]. Modulus profiling results for the nitrile rubber material [9] discussed earlier (fig. 3) are shown for aging at 125 °C (fig. 13) and at 80 °C

(fig. 14). The samples are 2 mm thick and P represents the percentage of the distance from one air-exposed surface to the opposite air-exposed surface. The unaged material has a uniform modulus of ~4 MPa across the cross-section. Aging at 125 °C leads to a heterogeneous profile caused by important DLO effects. Since the oxygen concentration at the sample surface is the true equilibrium sorption value, the modulus values at the surface represent the material degradation that would occur in the absence of DLO effects. DLO leads to drops in absorbed oxygen concentration with depth into the material and therefore less hardening (oxidative damage). The results at the much lower aging temperature of 80 °C show relatively uniform increases in modulus; this implies that DLO effects have essentially disappeared.

It might seem surprising that a material with large, temperature-dependent DLO effects occurring over its accelerated aging temperature range would exhibit such nearly perfect t-T superposition of its tensile elongation values (fig. 4) indicative of similar degradation shapes. It turns out fortuitously, that for many elastomers, elongation is often unaffected by DLO effects because oxidation typically leads to modulus increases (hardening) of the material. When DLO effects occur, the oxidation rate at the surface still proceeds under equilibrium oxygen



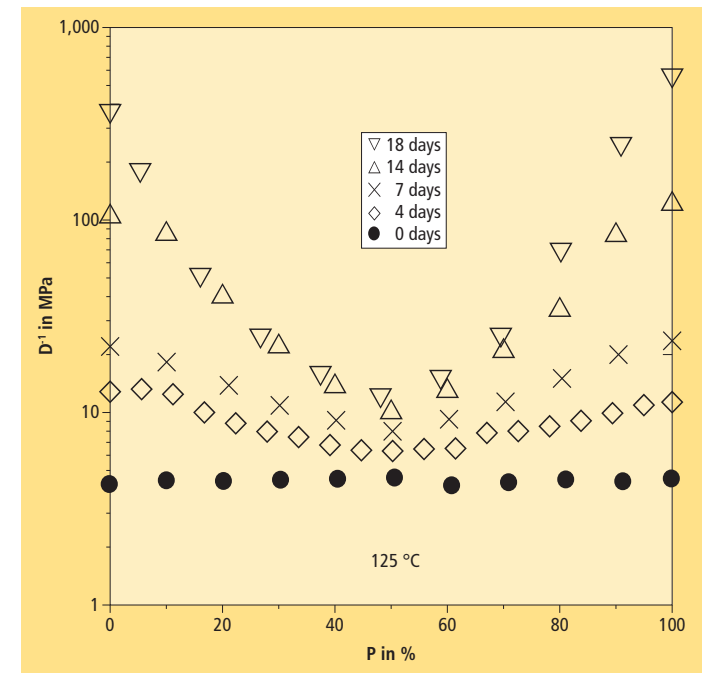
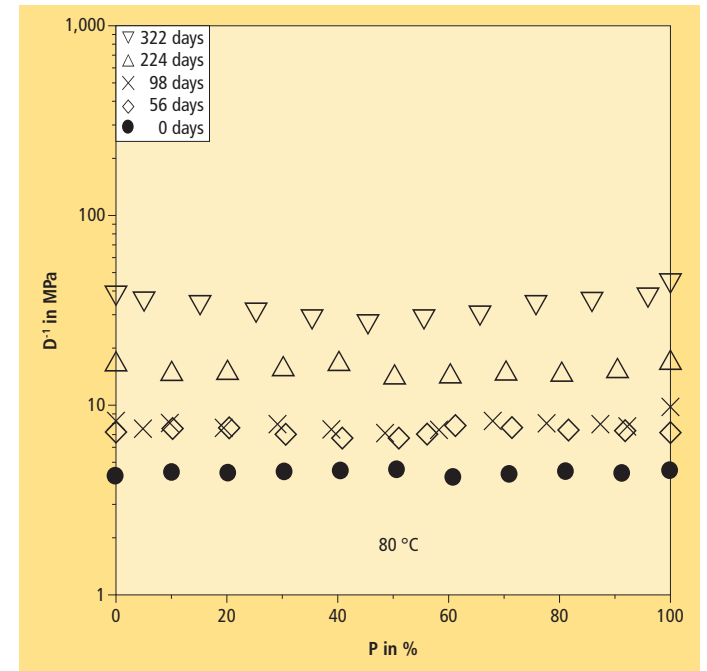


Fig. 14: Modulus profiles for nitrile rubber aged for the indicated times at 80 °C.



sorption conditions. This means that equilibrium hardening will still occur at the sample surfaces. When elongation measurements are carried out, cracks will invariably initiate at the hardened surfaces and, once initiated, these cracks are typically found to immediately propagate through the remainder of the sample cross-section. The hardened surface thus determines the elongation behavior, resulting in a relative insensitivity of tensile elongation to DLO effects at least for aging of many elastomers [1, 9, 17, 18, 19].

Although tensile elongation is often uninfluenced by DLO effects, other material properties that average across the cross-section of a material will show anomalous, un-interpretable convoluted behavior due to DLO. For instance, tensile strength (TS) data is available from the same experiments that obtain tensile elongation results but TS relates to force averages across the entire cross-section. The nitrile TS data [9] shifted with the same shift factors as those found for the elongation results are shown in **figure 15**. It is clear that DLO effects lead to non-superposable, basically un-interpretable TS data.

A second example of the problems caused by DLO effects is demonstrated for compression stress relaxation (CSR) studies on a commercial butyl seal material (Parker B612-70) [20]. Standard CSR experiments were done in both nitrogen and air using a standard 12.7 mm diameter cylindrical sample squeezed 25 % (therefore a 14.7 mm diameter cylinder when squeezed). The normalized force versus aging time at 125 °C for the 14.7 mm diameter samples aged in nitrogen and air is shown in **figure 16** and indicates that, as is usually the case, oxidation dominates the loss in force. Since the

force is integrated across the entire cylindrical cross-section, important DLO effects will be expected to retard the loss in force. DLO modeling of the cylindrical geometry [20] shows that DLO effects are important for the 14.7 mm diameter sample. To eliminate DLO, numerous smaller diameter disks (2 mm diameter at 125 °C) were squeezed and aged in parallel with the results shown on figure 16. To further illustrate the challenges associated with DLO effects, figure 17 com-

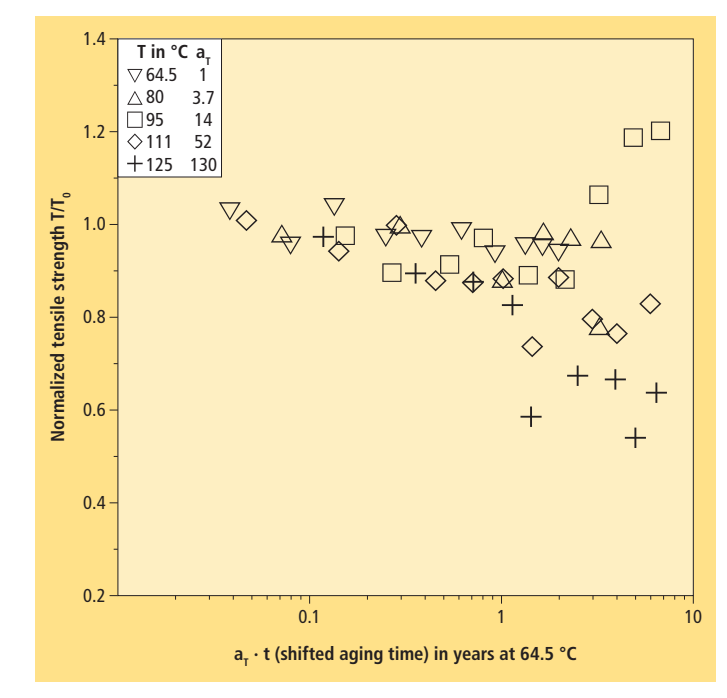


Fig. 15:
Time-temperature superposition of nitrile tensile strength results using the same shift factors found for elongation results.

Fig. 16: CSR force decay for a commercial Parker B612-70 butyl sealing material as a function of aging time at 125 $^{\circ}$ C

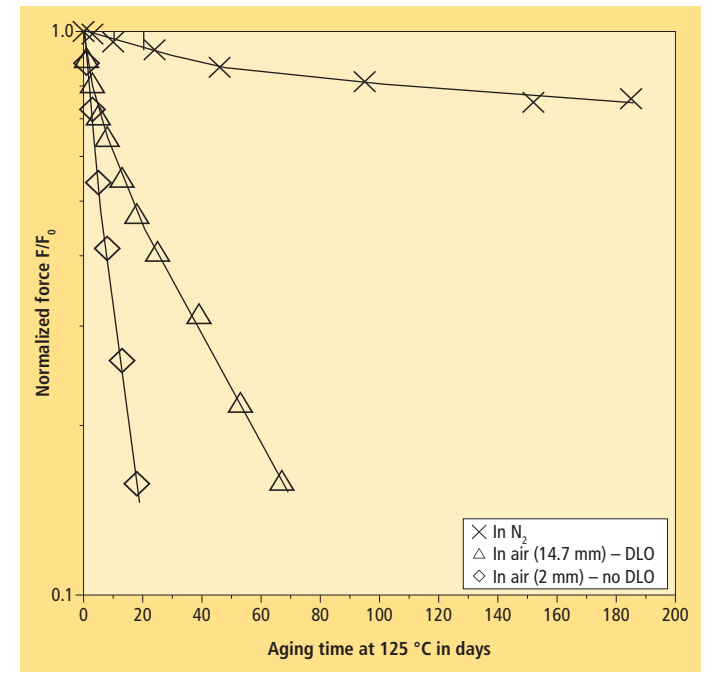
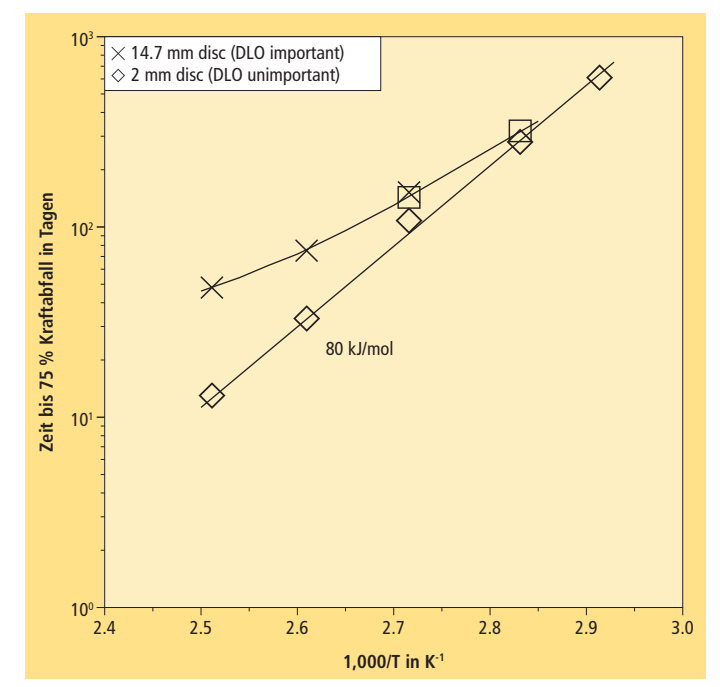


Fig. 17: Arrhenius plots for the Parker butyl seal of the times to 75 % force loss for the indicated conditions



pares Arrhenius plots of the time to 75 % loss in sealing force for the 14.7 mm and the 2 mm diameter samples. Even though the curving line for the 14.7 mm samples appears to eventually approach the proper results at low temperatures where DLO effects become small, it would be difficult to interpret the results and feel confident in attempting an extrapolation. This is not the case for the 2 mm results where DLO anomalies have been eliminated.

To be continued in Rubber Fibers Plastics 2 2017.

References

- [1] K. T. Gillen, M. Celina, R. L. Clough, and J. Wise, Trends in Polymer Science 5, 250 (1997).
- [2] A. V. Cunliffe and A. Davis, Polym. Degrad. Stab. 4, 17 (1982).

- [3] K. T. Gillen and R. L. Clough, Polymer 33, 4358 (1992).
- [4] L. Audouin, V. Langlois, J. Verdu, and J. C. M. DeBruijn, J. Mater. Sci. 29, 569 (1994).
- [5] L. M. Rincon-Rubio, X. Colin, L. Audouin, and J. Verdu, Rubber Chem. Technol. 76, 460 (2003).
- [6] M. C. Celina, Polym. Degrad. Stab. 98, 2419 (2013).
- [7] K. T. Gillen and R. L. Clough, Polym. Degrad. Stab. 24, 137 (1989).
- [8] J. D. Ferry, "Viscoelastic Properties of Polymers", John Wiley and Sons, 1970.
- [9] J. Wise, K. T. Gillen, and R. L. Clough, Polym. Degrad. Stab. 49, 403 (1995).
- [10] K. T. Gillen, R. Bernstein, R. L. Clough, and M. Celina, Polym. Degrad. Stab. 91, 2146 (2006).
- [11] K. T. Gillen, R. A. Assink, and R. Bernstein, "Nuclear Energy Plant Optimization (NEPO) Final Report on Aging and Condition Monitoring of Low-Voltage Cable Materials", Sandia Report, SAND2005-7331 (November, 2005).
- [12] J. Wise, K. T. Gillen, and R. L. Clough, Polymer

- 38, 1929 (1997).
- [13] J. Wise, K. T. Gillen, and R. L. Clough, Radiat. Phys. Chem. 49, 565 (1997).
- [14] M. Celina and K. T. Gillen, Macromolecules 38, 2754 (2005).
- [15] K. T. Gillen and R. L. Clough, "Techniques for Monitoring Heterogeneous Oxidation of Polymers", in Handbook of Polymer Science and Technology, Vol. 2, Ch. 6, N. P. Cheremisinoff, Ed., Marcel Dekker, New York, 1989.
- [16] K. T. Gillen, R. L. Clough, and C. A. Quintana, Polym. Degrad. Stab. 17, 31 (1987).
- [17] K. T. Gillen, E. R. Terrill, and R. W. Winter, Rubber Reviews. 74, 428 (2001).
- [18] M. Celina, J. Wise, D. K. Ottesen, K. T. Gillen, and R. L. Clough, Polym. Degrad. Stab. 68, 171 (2000).
- [19] K. T. Gillen, R. A. Assink, R. Bernstein, and M. Celina, Polym. Degrad. Stab. 91, 1273 1288 (2006).
- [20] K. T. Gillen, M. Celina, and M. R. Keenan, Rubber Chem. Technol. 73, 265 (2000).

The challenges of accelerated aging techniques for elastomer lifetime predictions – Part 2

K. T. Gillen, R. Bernstein, M. Celina

Elastomers are often degraded when exposed to air or high humidity for extended time periods (years to decades). Lifetime estimates normally involve extrapolating accelerated aging results made at higher than ambient environments. Several potential problems associated with such studies are reviewed and experimental/theoretical methods to address them are provided. The importance of verifying time-temperature superposition of degradation data is emphasized as evidence that the overall nature of the degradation process remains unchanged versus acceleration temperature. The confounding effects that occur when diffusion-limited oxidation (DLO) contributes under accelerated conditions are described and it is shown that the DLO magnitude can be modeled by measurements or estimates of oxygen permeability coefficients (P_{0x}) and oxygen consumption rates (ϕ) . P_{0x} and ϕ measurements can be influenced by DLO and it is demonstrated how confident values can be derived. Additionally, several experimental profiling techniques that screen for DLO effects are discussed. Values of ϕ taken from high temperature to temperatures approaching ambient can be used to more confidently extrapolate accelerated aging results for air-aged materials and many studies now show that Arrhenius extrapolations bend to lower activation energies as aging temperatures are lowered. Best approaches for accelerated aging extrapolations of humidity-exposed materials are also offered. Part 1 (RFP 1 2017) has covered the time-temperature superposition approach (chapter 2) and diffusion-limited oxidation (DLO) complications (chapter 3). Part 2 discusses O2 consumption measurements to model DLO and test extrapolations (chapter 4) and predicting lifetimes for humidity sensitive elastomers (chapter 5).

4 O₂ consumption measurements to model DLO and test extrapolations

We saw above that modeling of DLO effects requires measurements or estimates of the oxygen consumption rate ϕ under the environment of interest. We will see below that measurements of ϕ at temperatures in

Kenneth T. Gillen dandkgillen@comcast.net Robert Bernstein, Mat Celina

Sandia National Laboratories, Albuquerque, NM, USA

Published with kind permission of The Rubber Division, American Chemical Society, Inc.; Akron, OH, USA

the extrapolation temperature regime can offer more confident extrapolated predictions from high-temperature accelerated aging data. With the above in mind, we developed two different experimental approaches for measuring φ that had sensitivity sufficient to probe very low temperature conditions. The first approach [9] involves aging a polymer in a container with a known amount of oxygen and periodically determining the amount of oxygen consumed through gas chromatographic analyses. The second approach [21] is experimentally similar but uses a fuel cell detector to quantify the loss of oxygen. As will be seen below, these approaches are easily capable of measuring φ values down to 1 · 10⁻¹³ mol/g/s or even lower. It should be noted that DLO can also affect these measurements of ϕ , especially at higher temperatures. This problem must be addressed in the experimental procedure for which the polymeric samples need to be cut into sufficiently thin cross-sections to guarantee the elimination of DLO anomalies [9].

Given knowledge of the typical amount of oxidation necessary to significantly degrade polymeric materials, it can be shown that the sensitivity available from oxygen consumption measuring techniques $(1 \cdot 10^{-13} \text{ mol/g/s})$ implies the capability of measuring ϕ at temperatures corresponding to very long polymer lifetimes. For instance, the total oxygen absorption necessary to drop the elongation of the nitrile material during oven aging from 570 % to 100 % is $\sim 7 \cdot 10^{-4}$ mol/g [9]. A commercial chloroprene rubber cable jacketing material under oven aging conditions requires $\sim 5 \cdot 10^{-4}$ mol/g to drop the elongation from 296 % to 100 % [22]. Oxidative degradation to 100 % elongation under gamma radiation environments requires oxygen amounts of ~2.5 · 10⁻⁴ mol/g for commercial EPR materials, $\sim 5 \cdot 10^{-4}$ to $1 \cdot 10^{-3}$ mol/g for commercial chlorosulfonated polyethylene materials and ~7 · 10⁻⁴ mol/g for a commercial Brandrex XLPO cable jacketing material [23]. If it is assumed that a range of $2 \cdot 10^{-4}$ mol/g to $1 \cdot 10^{-3}$ mol/g (equivalent to 0.64 to 3.2 mass % oxidation) is necessary to cause significant damage over a 70 year polymer lifetime, the sensitivity needed for ϕ measurements is calculated to be $\sim 0.9 \cdot 10^{-13}$ mol/q/s to $4.5 \cdot 10^{-13}$ mol/g/s. Therefore the sensitivity of this technique (better than $1 \cdot 10^{-13}$ mol/g/s) allows probing the normal extrapolation regime down to temperatures corresponding to very long lifetimes.

The importance of DLO under ambient temperature conditions corresponding to a long elastomer lifetime of 70 years can be estimated using **equation 2** by obtaining estimates of ϕ and P_{Ox} . P_{Ox} values for most elastomers at lower temperatures range from $1 \cdot 10^{-10}$ to $1 \cdot 10^{-9}$ ccSTP/cm/s/cmHg (fig. 12) [14]. By combining this range of values with the expected range of ϕ for 70 year lifetimes $(0.9 \cdot 10^{-13} \text{ mol/g/s})$ to $4.5 \cdot 10^{-13} \text{ mol/g/s})$, **equation 2** leads to L_{90} values ranging from a low of \sim 6 mm to a high of \sim 38 mm. Such values imply that DLO effects will typically be completely absent for elastomers under their ambient aging conditions [6].

$$L_{90} \approx \left[\frac{kpP_{0x}}{\varphi} \right]^{0.5} \label{eq:L90}$$

It is also interesting to apply **equation 2** to the nitrile material for which modulus pro-

file results at 125 °C and 80 °C were shown in figure 13 and figure 14, respectively. For this material, values of ϕ (4 · 10⁻¹¹ mol/ g/s measured at 80 °C and 1.1 · 10-9 mol/ g/s estimated at 125 °C) and values for P_{0x} (2 · 10⁻⁹ ccSTP/cm/s/cmHg at 80 °C and 5.2 · 10⁻⁹ ccSTP/cm/s/cmHg at 125 °C, ccSTP: cubic centimeters of gas at standard temperature and pressure) were obtained [12]. These results coupled with equation 2, a sample density of 1.18 g/cm³ and an Albuquerque oxygen partial pressure of 13.2 cmHg, lead to L₉₀ values of 0.7 mm at 125 °C and 2.2 mm at 80 °C. Since the nitrile samples are ~2 mm thick, the results calculated from equation 2 are clearly in accord with the modulus profiling results given above.

Although we have shown that the use of equation 2 is consistent with the modulus profiling results for the nitrile rubber material, modeling of DLO can be rigorously applied to the nitrile modulus profile results to show reasonable quantitative agreement between the modeling shapes and the experimental shapes of the profiles versus aging time and temperature [12]. Similar quantitative agreement between theoretical and experimental profile shapes has been demonstrated for carbonyl profiles of an oven-aged chloroprene [18] and a nitrile rubber [24], for density profiles of an EPDM seal aged in radiation [3], and for modulus profiles of a Viton rubber aged in radiation environments [13].

These successful comparisons between theoretical and experimental profile shapes give confidence to the modeling and therefore to the use of equation 2 as an initial screening tool to make estimates of the likely importance of DLO effects for a material of given thickness in a particular aging environment. For instance, let us assume we had a 2 mm thick sheet of an elastomer whose tensile elongation dropped to 25 % of initial after 1 week of aging in a 125 °C oven and after 6 months of aging at 90 °C. Even if nothing is known about the ϕ and P_{0x} values at 125 °C and 90 °C, a reasonable first estimate of the importance of DLO under the two aging conditions can be obtained. Using 6 · 10-4 mol/g of oxygen to reach 25 % of initial elongation in 1 week and in 6 months leads to rough approximations for ϕ of $1 \cdot 10^{-9}$ mol/g/s (at 125 °C) and $3.8 \cdot 10^{-11}$ mol/g/s (at 90 °C). First crude estimates of P_{0x}, obtained from figure 12, are 7 · 10⁻⁹ ccSTP/cm/s/cmHg (at 125 °C) and 3 · 10⁻⁹ ccSTP/cm/s/cmHg (at 90 °C). Assuming a material density of 1 g/cm³ and sealevel oxygen partial pressure of 16 cmHg, equation 2 gives L₉₀ estimates of 1.0 mm (at 125 °C) and 3.4 mm (at 90 °C). These results suggest that DLO for the 2 mm thick elastomer would probably be important at 125 °C but not at 90 °C. If better estimates of ϕ and P_{0x} could be obtained from the literature or from experiments, such estimates could be improved. Some profiling experiments on the aged samples could further confirm such preliminary conclusions. One quick conclusion from such calculations is that important DLO effects might be anticipated for exposure environments that significantly degrade a 2 mm thick material in the weeks to several months timeframe. Since most accelerated aging experiments use temperature ranges that encompass weeks to several months degradation times, DLO effects are typically to be expected and should be checked for. Note also that a reduction in sample thickness during aging is one method of reducing or eliminating the importance of DLO effects, as was discussed earlier for CSR experiments.

Since equation 2 was used to show its consistency with profiling results and its utility for estimating when DLO effects become important, we now turn our attention to the use of the sensitive oxygen consumption methods as a means of gaining more confidence in extrapolations of higher temperature accelerated aging results. As noted in the discussion of figure 2, if non-Arrhenius behavior is found as the temperature is lowered, one would expect curvature towards lower Ea values. In certain instances, evidence of such drops in E_a values is observed by following the same degradation parameter to low enough aging temperatures. For example, elongation versus aging time results at five aging temperatures (121 °C to 70 °C) were obtained for a chloroprene cable jacketing material starting around January of 1979. We kept un-exposed samples in our lab (average temperature of ~ 24 °C) and tensile tested some samples in early 1998 and others in mid 2002, resulting in 19 and 23.6 year exposures at ~24 °C. All of the elongation results are shown in figure 18 [22]. Time-temperature superposition of these results is given in figure 19 and an Arrhenius plot of the shift factors is shown in figure 20. A clear drop in Arrhenius E_a from ~89 kJ/mol to ~71 kJ/mol occurs at lower temperatures. This relatively small change in slope causes a prediction of 96 years to reach 50 % elongation at 24 °C (based on extrapolation of the 89 kJ/mol E_a) to drop by 73 % to 36 years. Another example of an observation of a slope change from a single type of data (elongation again) comes from chlorosulfonated polyethylene (CSPE) mate-

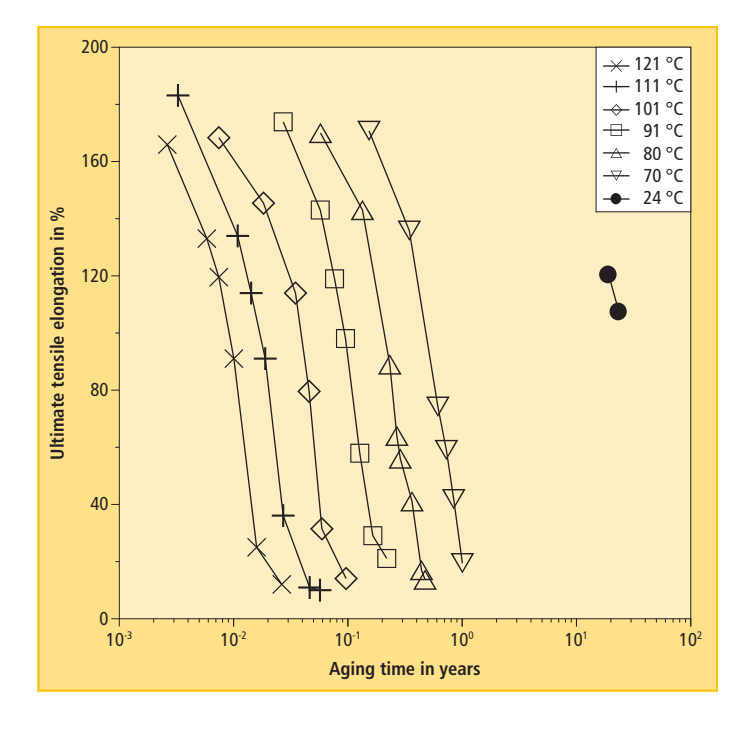


Fig. 18: Tensile elongation results for Okonite chloroprene material

rials, some of which were aged for as long as 5 years at 70 °C [19]. These results, shown in figure 21 again clearly indicate a drop in $\rm E_a$ at lower aging temperatures. Similar curvature in Arrhenius plots can also be obtained from oxidation rate measurements [25].

In most instances we do not have a sufficient range of accelerated aging data to observe changes in E_a and having long-term results such as the 23 year data at 24 °C for the chloroprene material or the 5 year data at 70 °C for the CSPE materials is unusual. Fortunately, there is another method that allows us to probe the low temperature regions to determine whether the E_a values derived at elevated temperatures change slope at lower temperatures. Oxy-

gen consumption is an approach where we earlier showed that the sensitivity allows for probing aging temperatures where materials would be expected to have 50 to 100 year lifetimes or longer. When oxygen is present during the degradation of most polymeric materials, oxidation processes normally dominate the chemical reactions so oxygen consumption rates ϕ are expected to be

Fig. 19: Time-temperature superposition at 24 °C for the chloroprene data from figure 18

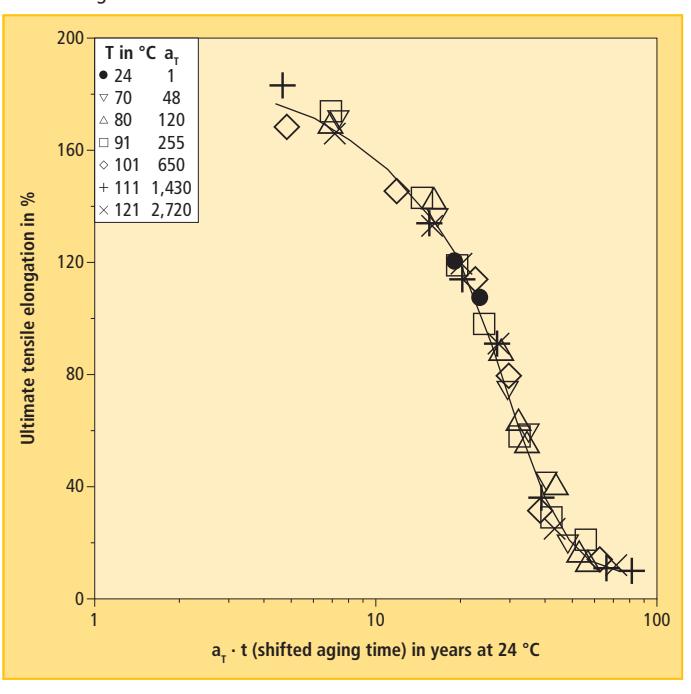


Fig. 21: Arrhenius plots of shift factors from elongation results for eight different commercial CSPE materials

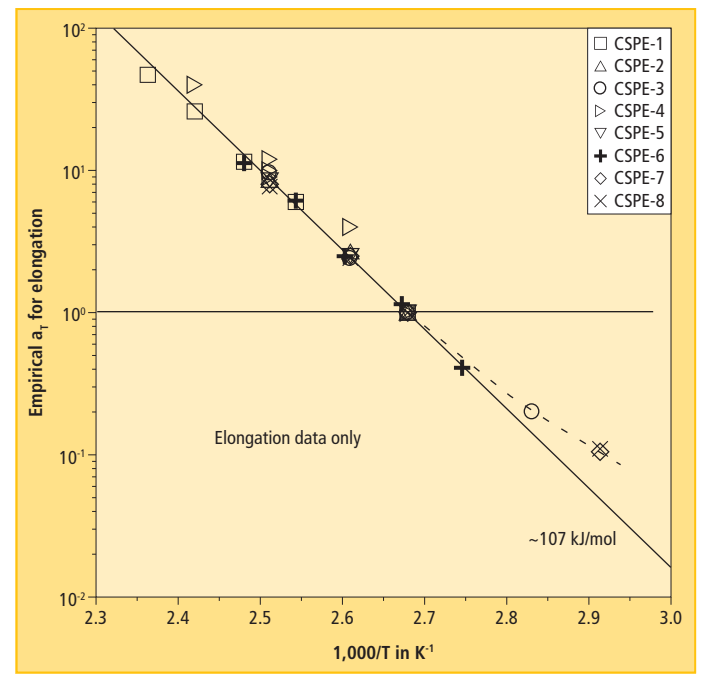


Fig. 20: Arrhenius plot of chloroprene shift factors from figure 19

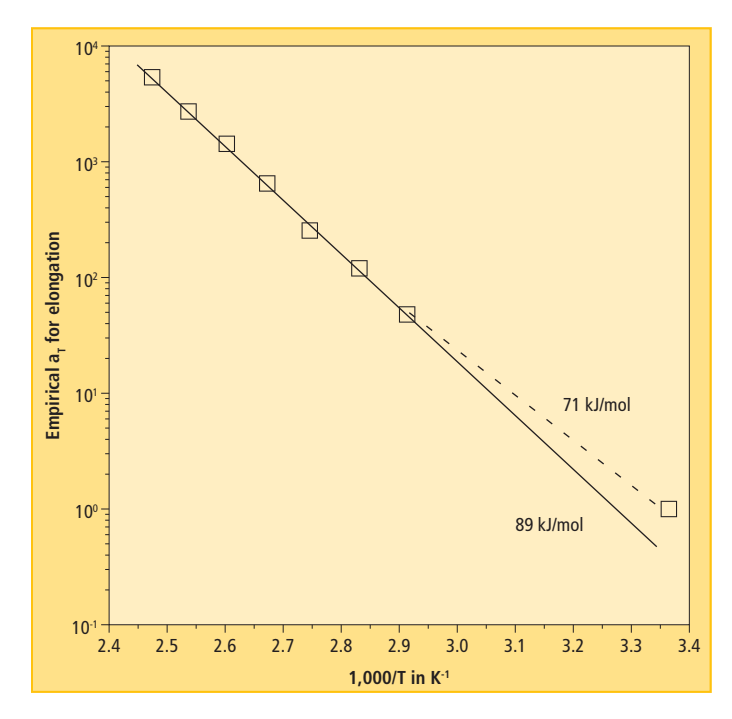
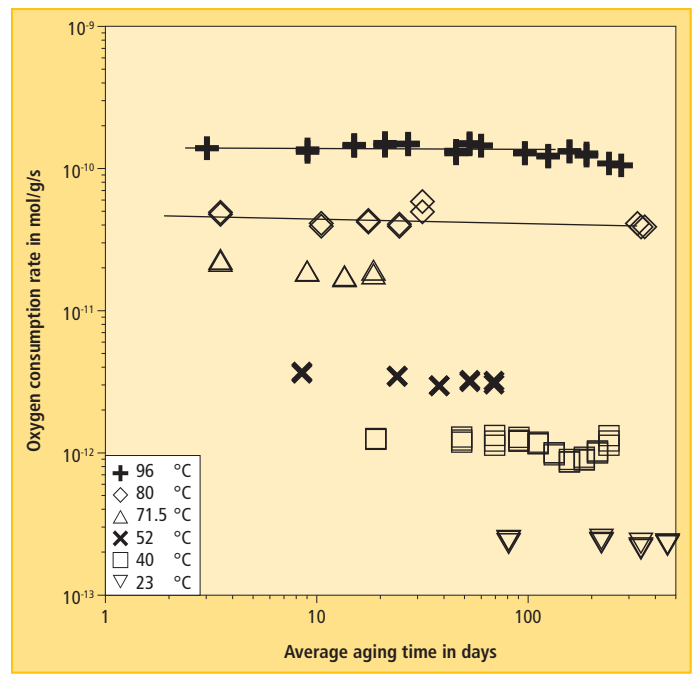


Fig. 22: $\;\;\varphi$ versus aging time for the nitrile rubber material at the indicated aging temperatures



correlated with loss of mechanical properties. By making ϕ measurements at higher temperatures that overlap the temperature range used for traditional mechanical property measurements, it is possible to confirm/ test the correlation between oxygen consumption and traditional (e.g., mechanical property) measurements. Extending the ϕ measurements into the extrapolation region then allows determining whether the oxidation mechanism changes or remains constant in this region. Oxygen consumption rate measurements [9] for the nitrile rubber material (fig. 3) are plotted versus aging time at the indicated aging temperatures in figure 22. The measurements at the highest three temperatures overlap the temperature region used for the elongation measurements (fig. 3); measurements at the three lowest temperatures allow us to probe the extrapolation region of the Arrhenius plot for this material (fig. 5). Note that the approach allows measurements at room temperature (23 °C) and that the values at this temperature are $\sim 2.5 \cdot 10^{-13}$ mol/q/s, illustrating the sensitivity of the approach. These results are then integrated to give the oxygen consumed (oxidation level) versus aging time, shown in figure 23. These integrated consumption versus time results are then t-T superposed using a reference temperature of 23 °C in figure 24. Figure 25 summarizes the shift factors for elongation (from figure 4), for surface modulus and for oxygen consumption where the oxygen consumption shift factors are normalized to unity at 64.5 °C [26]. The results indicate a slight drop in E₂ at lower temperatures, indicative of some changes in the degradation chemistry. Further evidence for a change in chemistry is obtained from the gas chromatographic oxygen consumption approach which also detects CO2, the main product gas. At 96 °C, CO₂ production represents ~7 % of oxygen consumption dropping to ~1.5 % at 23 °C. This leads to an E_a for CO₂ production of ~120 kJ/mol [9]. Therefore (see hypothetical figure 2), the oxidative reaction leading to CO2 become less important as the temperature drops, which is likely related to the small drop in E_a from ~90 kJ/mol to 80 kJ/mol.

It was shown earlier that Arrhenius plots of shift data for eight CSPE materials displayed evidence for a drop in E_a from elongation results (fig. 21). Oxygen consumption results [27] for two of these CSPE materials confirm this drop in E_a as seen in figure 26 which combines the elongation and consumption results. Again data on CO₂ production offers further evidence of the changing

chemistry since the ratio of CO_2 produced to oxygen consumed drops from 20-25 % at high temperatures to ~7 % at the lowest temperature of 37 °C [27].

In figure 1 we showed induction time results for an EPDM rubber sealing material at temperatures from 155 °C to 111 °C. Oxygen consumption results were obtained over the temperature range from 160 °C to 52 °C, integrated and then t-T superposed [26]. The shift factor results for superposed elongation, density and oxygen consumption (normalized at 111 °C) are plotted in figure 27 and show a substantial change in Arrhenius slope below 111 °C. The E_a at high temperatures is 118 kJ/mol similar to the 116 kJ/mol found using induction time estimates (fig. 1). As is usually the case, the oxygen consumption E_a results that overlap the high temperature accelerated aging temperature range agree with the E_a results for mechanical property changes verifying the expectation that oxygen consumption is correlated with mechanical property changes. Since the oxygen consumption results only reach 52 °C (where φ is close to the experimental limit of $1 \cdot 10^{-13}$ mol/g/s), it is possible that the E₂ value might drop below 82 kJ/ mol at still lower temperatures. However, the extrapolation to 52 °C predicts already

Fig. 23: Integrated oxygen consumption versus aging time for the nitrile rubber. The two arrows indicate the consumption corresponding to the elongation dropping to 100 % from its initial 570 % (e/e $_0$ ~0.175 in figure 3).

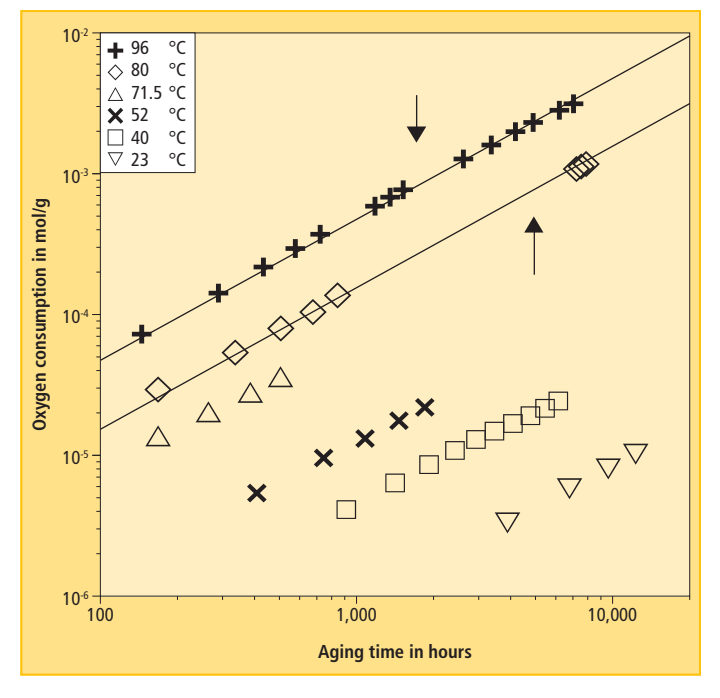
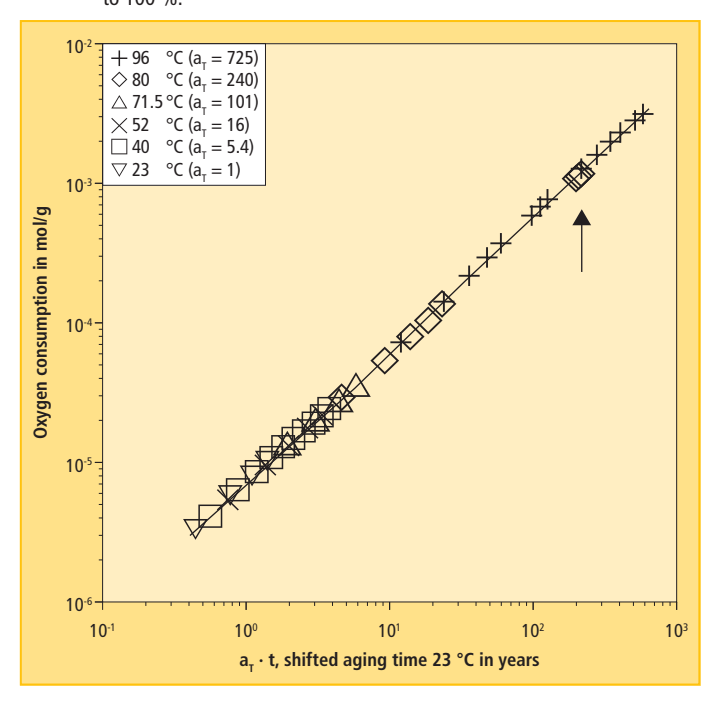


Fig. 24: t-T superposition of the consumption results from figure 23. The arrow indicates the consumption result corresponding to the elongation dropping to 100 %.



a lifetime of more than 100 years so clearly long life (but not 55,000 years) would be predicted for 25 $^{\circ}$ C.

Similar evidence for drops in E_a from both elongation results (down to 50 °C) and oxygen consumption measurements (down to 25 °C) for a polyurethane rubber material are shown in figure 28 [28].

A particularly interesting study [29] that semi-quantitatively verifies the predictions made using oxygen consumption measurements shows a comparison of results for two commercial butyl o-ring materials, a Parker B612-70 and a Burke 4061. The Parker sealing force data were shown in **figure 16** and **figure 17** during the discussion on DLO effects. The E_a determined in the absence of

DLO effects was 80 kJ/mol. Similar experiments were conducted for the Burke material with the results for both materials plotted in **figure 29**. Although the Burke material degrades faster at high temperatures, its Arrhenius E_a (~105 kJ/mol) is greater than that of the Parker material, so its predicted extrapolated lifetime at 23 °C is ~150 years versus ~63 years for the lower E_a Parker ma-

Fig. 25: Arrhenius plot of shift factors for elongation, surface modulus and oxygen consumption for nitrile rubber

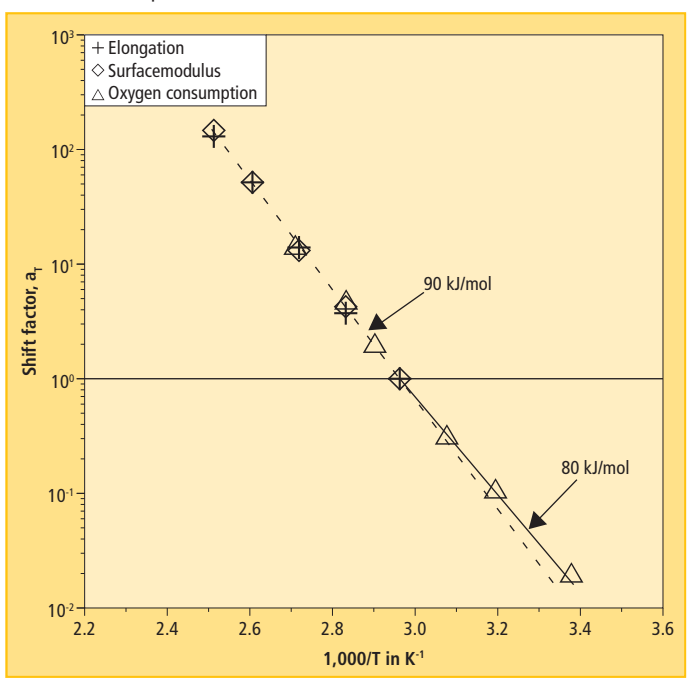


Fig. 27: Arrhenius plot of elongation, density and oxygen consumption shift fac-

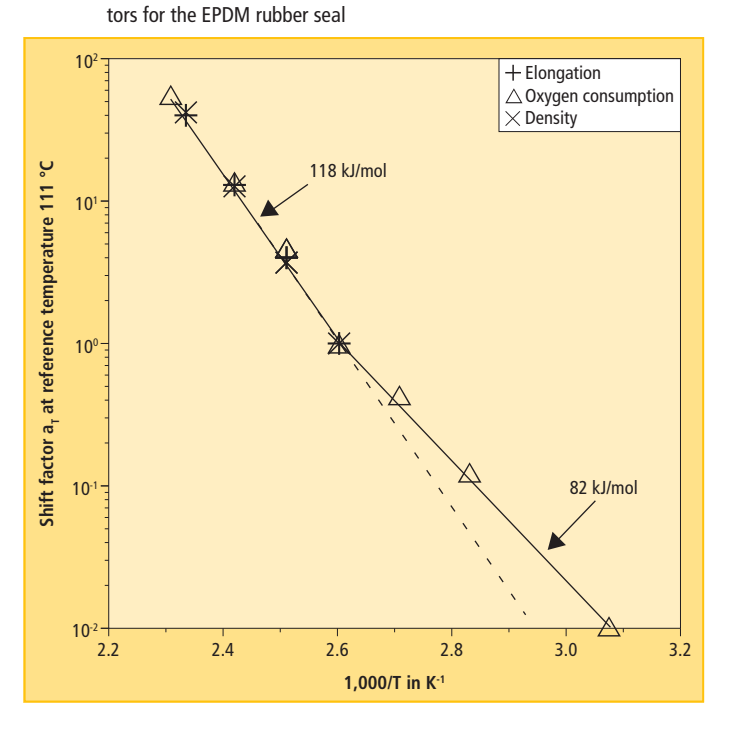


Fig. 26: Arrhenius plots of shift factors for elongation and oxygen consumption for CSPE materials

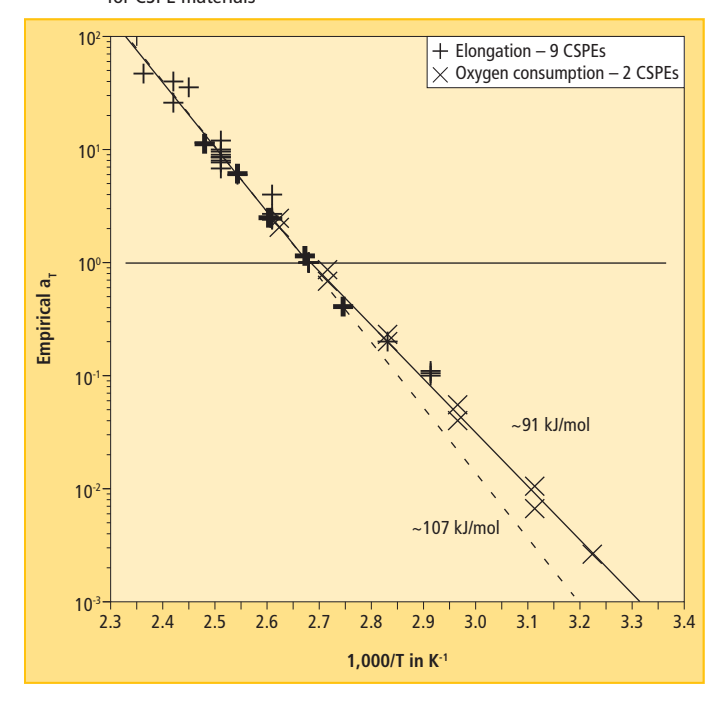
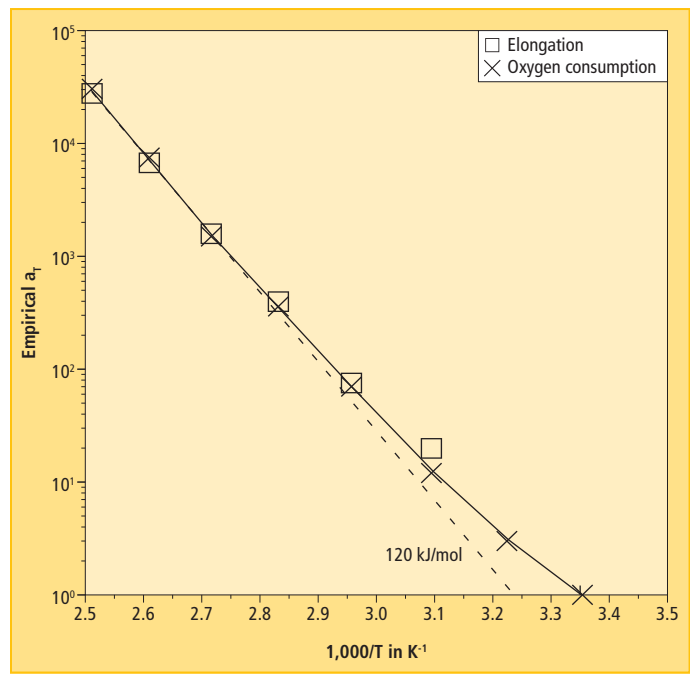


Fig. 28: Arrhenius plots of the shift factors from elongation and oxygen consumption for a polyurethane rubber



terial. Oxygen consumption results were run on these two materials from 110 °C to 25 °C and after analysis using t-T superposition in the usual way, the inverse of the shift factors were normalized to the results of **figure 29**, resulting in the extrapolated results shown in **figure 30**. There is a small curvature to lower E_a for the Parker material, reducing the predicted time to 50 % loss in force at 23 °C from 63 years to ~50 years. The drop in E_a for the Burke material is much larger,

reducing the predicted time to 50 % loss in force at 23 °C by an order of magnitude from 150 years to \sim 16 years. In this instance numerous samples were obtained of both materials aged as compressed o-ring seals in the field for 16 to 22 years at an estimated average temperature of 23 °C. The measured compression set values for the Burke o-rings were \sim 50 % \pm 15 % and those for the Parker o-rings were \sim 10 % \pm 10 % [29]. Since compression set values for these materials were

found to vary inversely with force loss values [30], the order of magnitude predicted drop in the Burke time to 50 % loss in force from the oxygen consumption results and the reversal of life predictions for the two materials was confirmed.

In documenting the many instances where Arrhenius plots show curvature to lower E₂ values at lower temperatures, we have concentrated on elastomeric materials. It turns out that similar evidence has been collected for many other polymeric materials. A review shows that such behavior has been noted for several additional materials [25]. For polypropylene, high temperature E₃ values often drop by factors of 2.5 to 4 around 60 °C to 80 °C. For one XLPO material, its high temperature E_a of 135 kJ/mol dropped to 98 kJ/mol at lower temperature whereas a second XLPO (the one described in figure 11) saw no change in its E_a value of 72 kJ/mol at lower temperatures [11]. A recent publication [31] followed the tensile strength of a nylon material aged in air for up to 5.5 years at temperature ranging from 37 °C to 138 °C. The usual t-T analysis led to shift factors that indicated an E_a of 96 kJ/mol above ~100 °C which dropped by a factor of more than three times to 30 kJ/mol at lower temperatures, as shown in figure 31. It is thus clear from the results presented in this review that curvature to lower E_a values is commonly

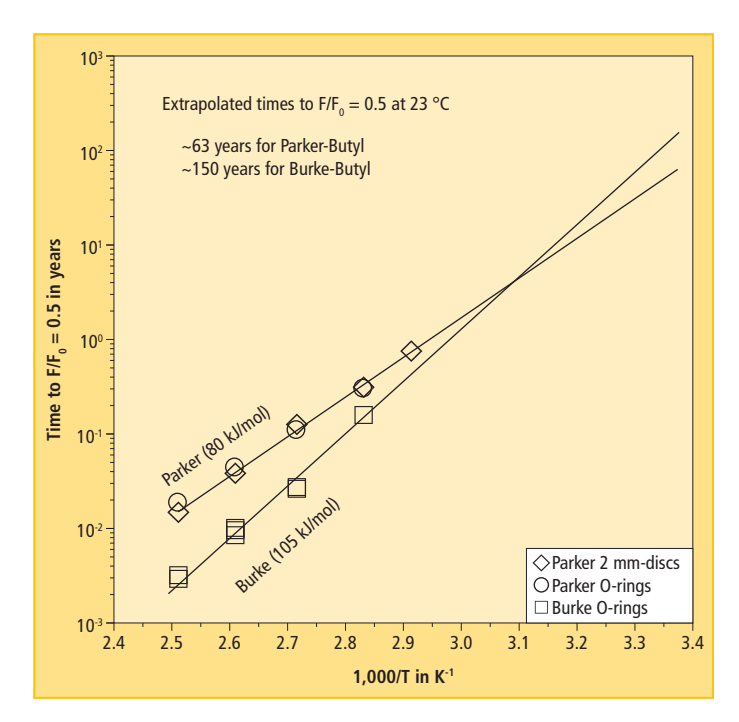


Fig. 29: Arrhenius plot of the times to 50 % loss in sealing force for two butyl rubber materials

Fig. 30: Arrhenius plot of figure 29 with added results from oxygen consumption experiments

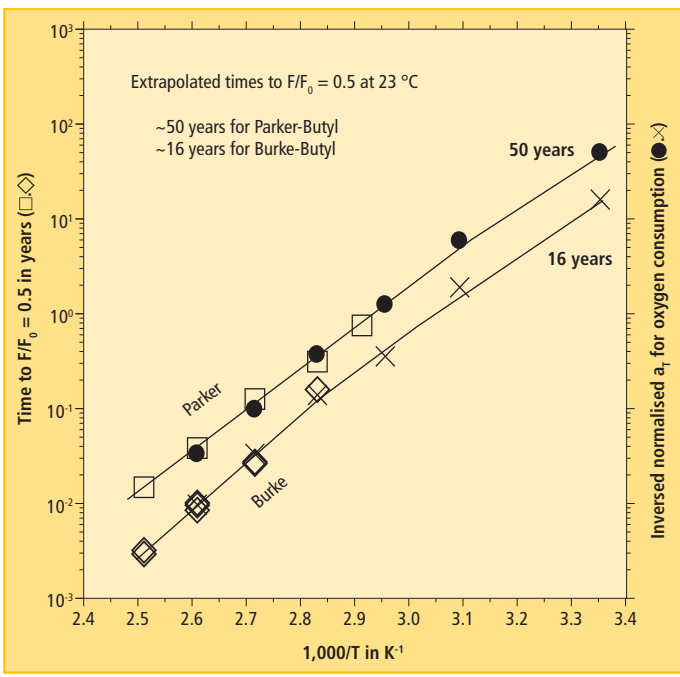
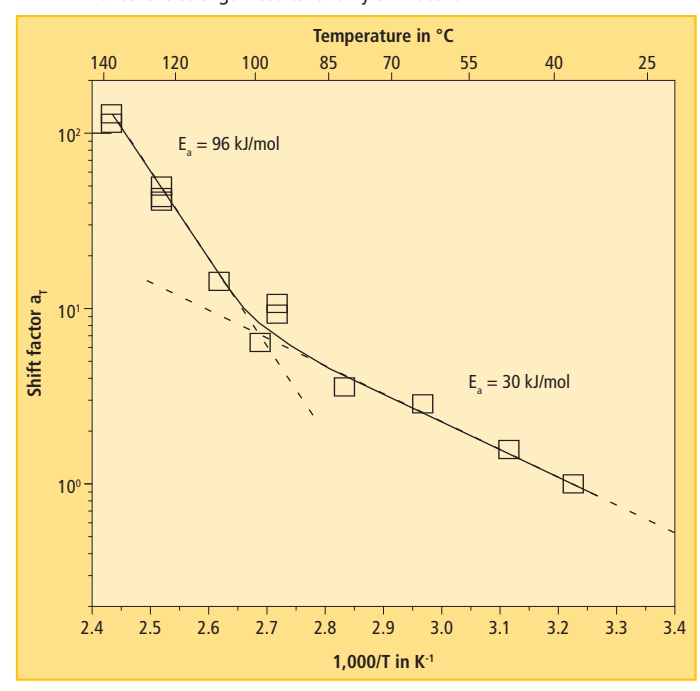


Fig. 31: Arrhenius plot of the shift factors derived from t-T superposition analysis of tensile strength results for a nylon material



observed for most polymeric materials and often confirmed when long-term aged samples are available for study.

Although there is no need to understand the often complex chemical mechanisms causing the drop in E₂ values in order to make better predictions at low temperatures, elucidating the chemistry can be useful since such knowledge may allow improvements in formulations leading to enhanced lifetimes. One general explanation for the drop in E_a values at lower temperatures is based on the fact that segmental mobility of termination processes is less efficient when the temperature decreases [32]. For materials where the CO₂ gas production increases substantially as the temperature increases such as for the nitrile rubber [9] and CSPE materials [27] mentioned earlier, Le Gac and co-workers [33] conclude that the CO₂ must come from secondary processes involving very unstable structures such as secondary hydroperoxides. Therefore this mechanism must become more important at higher temperatures.

5 Predicting lifetimes for humidity sensitive Elastomers

A more detailed description of the subject is given in [34]. Sorption isotherms for a gas

show how the dependence of the solubility of the gas at equilibrium in the material depends on the partial pressure of the gas surrounding the material. For oxygen up to normal atmospheric pressure, the isotherms for most materials are linear. For condensable gases like water, the isotherms are more complex, typically increasing as the water vapor pressure approaches 100 % relative humidity (RH) at a given temperature. Some typical results [35] for a silicone rubber (poly-3,3,3-trifluoropropylmethyl-phenylsiloxane, abbreviated FMS) are plotted versus T and RH in figure 32. At each temperature, the sorption isotherm results are reasonably linear up to ~50 % RH, but start to climb more and more rapidly at higher RH values. A log plot of the water sorption values at constant RH values of 20 %, 40 %, 60 % and 80 % versus inverse absolute temperature (an Arrhenius-like plot) shows approximately linear behavior at each RH, and the Arrhenius slopes are approximately parallel with an $E_{a(RH)}$ of ~21 kJ/mol (fig. 33).

Similar behavior is found for water sorption isotherms in many elastomeric materials although the region of a break from approximate linearity may vary. For instance, Barrie and Machin [35] also present water sorption isotherms for two additional silicone rubbers, polydimethyl-siloxane and polydimeth-

ylphenyl-siloxane that can be analyzed in a similar fashion and give parallel Arrhenius lines with slopes ~16 kJ/mol and 18 kJ/mol, respectively. Vieth and Amini [36] presented data for a polyurethane membrane where the sorption isotherms for water at 25 °C, 40 °C and 55 °C were identical implying an $E_{a(RH)}$ of 0 kJ/mol. Thus it appears that at a given constant RH, the solubility and hence the concentration of water in many elastomers has a small dependence on temperature that is approximately Arrhenius and that this Arrhenius dependence may be relatively constant at all values of RH.

The simplest kinetic representation of the reaction of two species A and B to give a degradation product D, follows **equation 3**.

$$\frac{dD}{dt} = k[A][B] = exp \left[\frac{-E_{a(thermal)}}{RT} \right] [A][B]$$
 3

[A] and [B] represent the concentration of the two reacting species and k represents the reaction rate constant which typically has an Arrhenius dependence on temperature as indicated. We will assume that the overall rate of the polymer (P) degradation under humidity conditions follows such an equation. Given that the water concentration dissolved in the polymer [H₂O] has an Arrhenius dependence

Fig. 32: Water sorption isotherms versus % RH for FMS, a silicone rubber

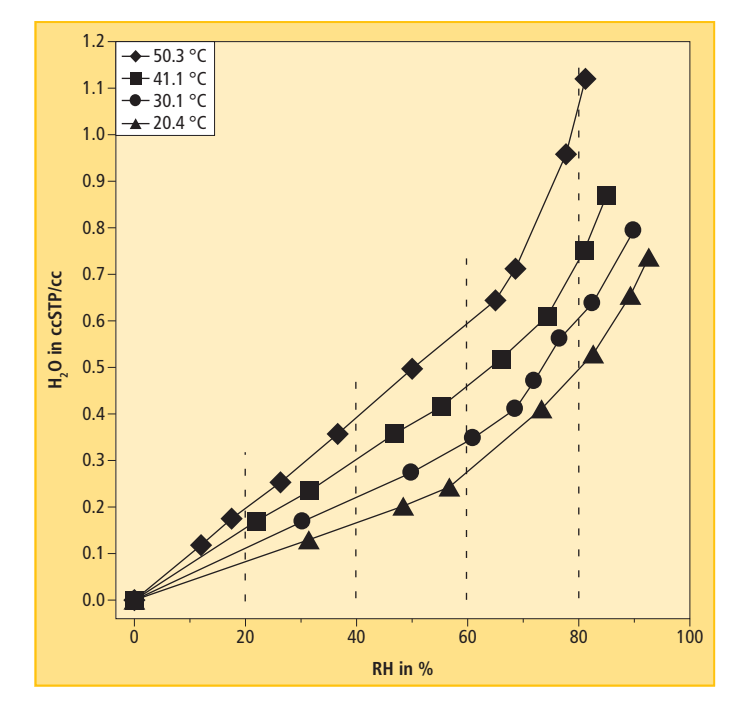
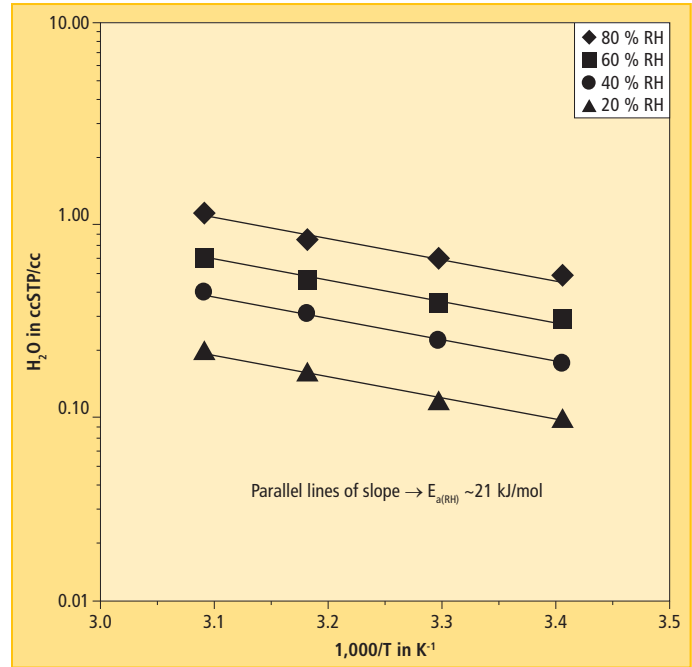


Fig. 33: Arrhenius plot of water sorption in the silicone material from figure 32 versus RH and inverse absolute T



at constant RH and that the concentration of polymer [P] will change very little with degradation, **equation 3** becomes the **equation 4** for humidity aging at constant [RH].

$$\begin{split} &\frac{dD}{dt} = k[H_2O][P] \propto \\ &\exp \left[-\frac{E_{a(thermal)}}{RT} \right] \exp \left[-\frac{E_{a(RH)}}{RT} \right] \propto \exp \left[-\frac{E_a - E_{RH}}{RT} \right] \quad & \textbf{4} \end{split}$$

These results suggest that if we carry out humidity aging experiments by varying the aging temperature under constant RH conditions, we might anticipate Arrhenius behavior with activation energy given by $E_a + E_{RH}$, an assumption that can be easily tested [25]. Welch [37] presented extensive data examining the reversion (from solid back to liquid) of a polyurethane potting compound versus aging temperature and RH. We analyzed Welch's data under constant RH conditions and observed parallel Arrhenius results with an activation energy of 89 kJ/mol, confirming the above approach (fig. 34). More recent results for a polyester [38], cellulose [39] and nylon 6,6 [31] found similar linearity for Arrhenius plots of degradation rates analyzed at constant RH. Once Arrhenius behavior is confirmed, it can be extrapolated to lower temperatures. But such extrapolations could be misinterpreted due to a lower activation energy process that contributes at low temperatures. For instance, in the nylon 6,6 study of tensile strength decay done both in air-aging ovens and at 100 % RH humidity, degradation at 100 % RH [31] dominated oxidative degradation at temperatures above 50 °C but with a higher E_a than the degradation caused during air aging (fig. 35). At temperatures below ~50 °C, the lower E_a reactions driving the oxidation degradation pathway would be expected to take over, offering an excellent example of the phenomenon described in figure 2. Note also the drop in E_a for air aging at around 100 °C, previously shown with superposition data in figure 31.

6 Conclusion

In this review, we discussed and offered possible solutions to several important concerns and challenges that occur when accelerated aging studies in air and humidity environments are analyzed and extrapolated for lifetime predictions under lower temperature or ambient aging conditions. We noted that any changes in the degradation 'chemistry' occurring as the aging and extrapolation temperature drops will normally

lead to a lower slope of the often-applied Arrhenius model. To better assess whether changes in chemistry are occurring with changes in temperature, we emphasized the use of time-temperature superposition procedures such that all aging data are used in the analyses. Potential complications caused by diffusion-limited oxidation (DLO) effects were discussed and a simple expression involving estimates or measurements of the oxygen consumption rate ϕ and the oxygen permeability coefficient Pox was shown to be useful for quick estimates of conditions leading to potential DLO effects. Even in the absence of any existing measurements of ϕ , we outlined a guiding approach based on the expectation of significant oxidative degradation corresponding to oxygen absorption of \sim (6±4) · 10⁻⁴ mol oxygen per gram of polymer. The use of material profiling techniques to identify the presence of DLO anomalies was described with particular emphasis on modulus profiling, a technique ideally suited to the aging of elastomers. Evidence was presented that described why surface sensitive degradation failures (e.g., elongation measurements) of elastomers are often unaffected by DLO effects whereas measurements sensitive to property averages across the whole material cross-section (e.g., tensile strength, sealing force decay) are pro-

Fig. 34: Arrhenius plots of the reversion times for a polyurethane material at constant RH values

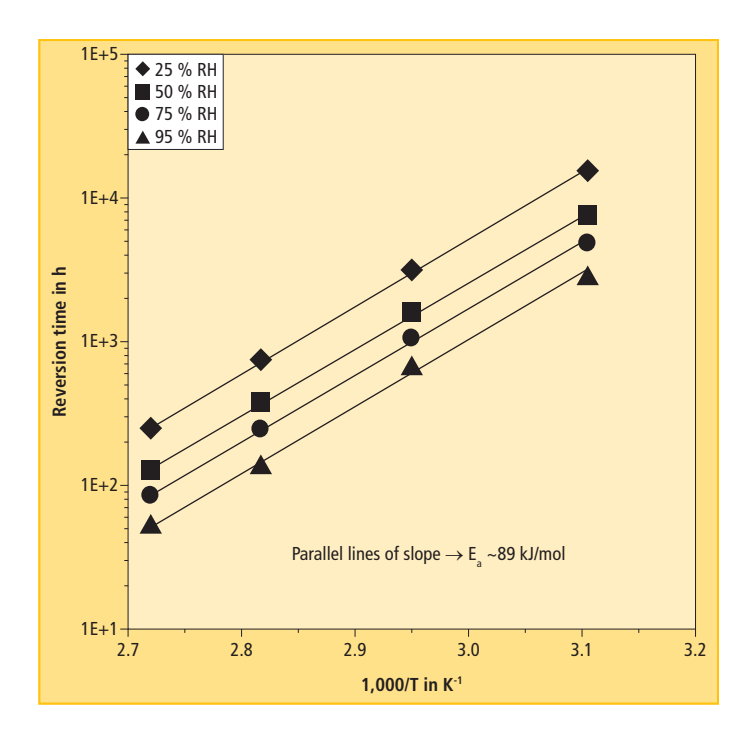
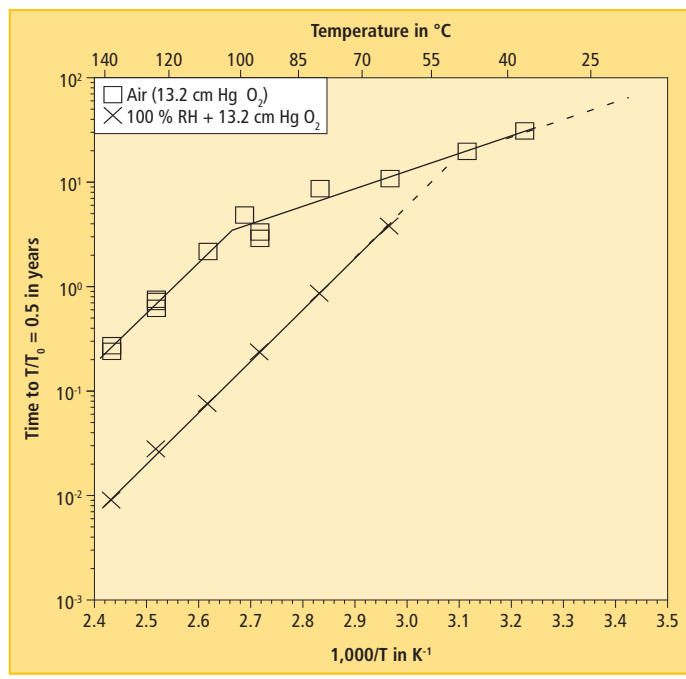


Fig. 35: Arrhenius plot of the time to 50 % loss in tensile strength for a nylon 6,6 material in air and in 100 % RH environments which also contain O_2 at the partial pressure operative in air in Albuquerque



foundly affected. Two methods for experimentally measuring ϕ were described and the sensitivity of these methods (oxidation rates $\leq 1 \cdot 10^{-13} \text{ mol/g/s}$) was shown to be sufficient to allow for measurements under temperature conditions where elastomers would have expected lifetimes of 50 to 100 years. This sensitivity led to the ability to use ϕ measurements as a means of gaining greater confidence in extrapolated predictions of accelerated aging results, as long as similar correlations between oxidation levels and mechanical property changes apply. Long-term aging experiments on several elastomers plus the use of ϕ measurements in the normal extrapolation regime for many elastomers showed that Arrhenius E_a values commonly dropped to lower values as the temperature was reduced, indicating changes in chemically driven degradation processes at lower temperatures for most materials. This implies a lowering of predicted polymer lifetimes. For a chloroprene rubber, such a change in slope was confirmed based on actual long-term aging results at 24 °C. For a butyl material the change in slope from φ data reduced the predicted time for a 50 % loss of sealing force at 23 °C by an order of magnitude to ~16 years, a prediction that was quantitatively confirmed from actual field-aged results out to 22 years. Finally, a simple concept is presented that leads to a reasonable approach for carrying out degradation predictions for materials sensitive to humidity aging effects, which recommends aging experiments at constant relative humidity conditions.

7 Acknowledgements

Sandia National Laboratories is a multimission laboratory managed and operated by Sandia Corporation, a wholly owned subsidiary of Lockheed Martin Corporation, for the U.S. Department of Energy's National Nuclear Security Administration under contract DE-AC04-94AL85000.

8 References

- [1] K. T. Gillen, M. Celina, R. L. Clough, and J. Wise, Trends in Polymer Science 5, 250 (1997).
- [2] A. V. Cunliffe and A. Davis, Polym. Degrad.

- Stab. 4, 17 (1982).
- [3] K. T. Gillen and R. L. Clough, Polymer 33, 4358 (1992).
- [4] L. Audouin, V. Langlois, J. Verdu, and J. C. M. DeBruijn, J. Mater. Sci. 29, 569 (1994).
- [5] L. M. Rincon-Rubio, X. Colin, L. Audouin, and J. Verdu, Rubber Chem. Technol. 76, 460 (2003).
- [6] M. C. Celina, Polym. Degrad. Stab. 98, 2419 (2013).
- [7] K. T. Gillen and R. L. Clough, Polym. Degrad. Stab. 24, 137 (1989).
- [8] J. D. Ferry, "Viscoelastic Properties of Polymers", John Wiley and Sons, 1970.
- [9] J. Wise, K. T. Gillen, and R. L. Clough, Polym. Degrad. Stab. 49, 403 (1995).
- [10] K. T. Gillen, R. Bernstein, R. L. Clough, and M. Celina, Polym. Degrad. Stab. 91, 2146 (2006).
- [11] K. T. Gillen, R. A. Assink, and R. Bernstein, "Nuclear Energy Plant Optimization (NEPO) Final Report on Aging and Condition Monitoring of Low-Voltage Cable Materials", Sandia Report, SAND2005-7331 (November, 2005).
- [12] J. Wise, K. T. Gillen, and R. L. Clough, Polymer 38, 1929 (1997).
- [13] J. Wise, K. T. Gillen, and R. L. Clough, Radiat. Phys. Chem. 49, 565 (1997).
- [14] M. Celina and K. T. Gillen, Macromolecules 38, 2754 (2005).
- [15] K. T. Gillen and R. L. Clough, "Techniques for Monitoring Heterogeneous Oxidation of Polymers", in Handbook of Polymer Science and Technology, Vol. 2, Ch. 6, N. P. Cheremisinoff, Ed., Marcel Dekker, New York, 1989.
- [16] K. T. Gillen, R. L. Clough, and C. A. Quintana, Polym. Degrad. Stab. 17, 31 (1987).
- [17] K. T. Gillen, E. R. Terrill, and R. W. Winter, Rubber Reviews. 74, 428 (2001).
- [18] M. Celina, J. Wise, D. K. Ottesen, K. T. Gillen, and R. L. Clough, Polym. Degrad. Stab. 68, 171 (2000).
- [19] K. T. Gillen, R. A. Assink, R. Bernstein, and M. Celina, Polym. Degrad. Stab. 91, 1273–1288 (2006).
- [20] K. T. Gillen, M. Celina, and M. R. Keenan, Rubber Chem. Technol. 73, 265 (2000).
- [21] R. A. Assink, M. Celina, J. M. Skutnik, and D. J. Harris, Polymer 46, 11648 (2005).
- [22] K. T. Gillen, R. Bernstein, and D. K. Derzon, Polym. Degrad. Stab. 87, 57 (2005).
- [23] M. C. Celina, K. T. Gillen, and E. R. Lindgren, "Nuclear Power Plant Cable Materials: Review of Qualification and Currently Available Aging Data for Margin Assessments in Cable Performance", Sandia Report, SAND2013-2388 (May, 2013).

- [24] M. C. Celina, J. Wise, D. K. Ottesen, K. T. Gillen and R. I. Clough, Polym. Degrad. Stab. 60, 493 (1998).
- [25] M. Celina, K. T. Gillen, and R. A. Assink, Polym. Degrad. Stab. 90, 395-404 (2005).
- [26] K. T. Gillen and M. Celina, Polym. Degrad. Stab. 71, 15 (2001).
- [27] K. T. Gillen, R. Bernstein, and M. Celina, Polym. Degrad. Stab. 87, 335 (2005).
- [28] M. Celina, A. C. Graham, K. T. Gillen, R. A. Assink, and L. M. Minier, Rubber Chem. Technol. 73, 678 (2000).
- [29] K. T. Gillen, M. Celina, and R. Bernstein, Polym. Degrad. Stab. 82, 25 (2003).
- [30] K. T. Gillen, R. Bernstein, and M. H. Wilson, Polym. Degrad. Stab. 87, 257 (2005).
- [31] R. Bernstein and K. T. Gillen, Polym. Degrad. Stab. 95, 1471 (2010).
- [32] N. Khelidj, X. Colin, L. Audouin, J. Verdu, C. Monchy-Leroy, and V. Pronier, Polym. Degrad. Stab. 91, 1598 (2006).
- [33] P. Y. Le Gac, G. Roux, J. Verdu, P. Davies and B. Fayolle, Polym. Degrad. Stab. 109, 175 (2014).
- [34] K. T. Gillen and K. E. Mead, "Predicting Life Expectancy and Simulating Age of Complex Equipment Using Accelerated Aging Techniques", Sandia Report, SAND79-1561 (January, 1980).
- [35] J. A. Barrie and D. Machin, J. Macromol. Sci. Phys. 83, 645 (1969).
- [36] W. R. Vieth and M. A. Amini, Polymer Science and Technology, Vol. 6, H. B. Hopfenberg, Ed., Plenum, New York (1974), p, 49.
- [37] G. L. Welch, National SAMPE Technical Conference Proceedings, Vol. 2, Aerospace Adhesives and Elastomers, Dallas, TX, 1970.
- [38] R. R. Dixon, Polym. Eng. Sci. 33, 65 (1993).
- [39] X. Zou, T. Uesaka, and N. Gurnagul, Cellulose 3, 243 (1996).

This article is based on a presentation given at the 186th Technical Meeting of the Rubber Division, American Chemical Society, Nashville, TN, USA, October 2014 (Rubber Chemistry and Technology 88/1 (2015), 1), which has been honored as best paper of the meeting.